TAMPEREEN TEKNILLINEN YLIOPISTO
TAMPERE UNIVERSITY OF TECHNOLOGY

NIMA RASHVAND

MODELLING & CRUISE CONTROL OF A MOBILE MACHINE WITH HYDROSTATIC POWER TRANSMISSION

MASTER OF SCIENCE THESIS

Examiners: Professor Kalevi Huhtala

Dr Reza Ghabcheloo

The thesis is approved at the faculty council meeting of automation, Mechanical and Materials Engineering on OCT,3, 2012

Abstract

TAMPERE UNIVERSITY OF TECHNOLOGY

Master's Degree program in Machine Automation

RASHVAND, NIMA: Modeling & cruise control of a mobile machine with hydrostatic power transmission

Master of Science Thesis, 84 pages, 9 Appendix pages

Major: Machine Automation

Examiner: Professor Kalevi Huhtala, Dr. Reza Ghabcheloo

Keywords: Hydrostatic power transmission, Longitudinal vehicle dynamic Volumetric & hydro mechanical efficiencies, Leakage flow, Simulation

A parallel hydrostatic power transmission is studied and the possible constraint which can effect on the fluid division in the system is analyzed.

The dynamic model of the machine is studied in two sections: a simplified model and a complicated model. In both of the models all the acting forces and their effect on the vehicle's motion are studied and the dynamic behavior of the machine is calculated using mathematical equations.

The speed of the machine cannot be controlled by a simple feedback control. It is concluded that a simple feedback controller does not provide the best performance for this application. The gain-scheduled PID controller is used for this application. This Type of controller can adapt itself with the variable dynamic characteristics of the hydraulic system.

Gain scheduling is the major key in gain-scheduled PID controller. The results of tuning with different gains are shown and the Bode & step diagrams are presented.

Several static tests on the machine have been done to monitor the behavior of the HST. For the first test the diesel engine rotational speed is kept constant at 1200 RPM and the displacement of hydraulic pump is modified. For the second test the displacement of hydraulic pump is kept constant at 60% and the diesel engine rotational speed RPM is modified. In both of the tests the vehicle is moved in a straight direction and on a smooth terrain.

The result of comparison between the open loop & closed loop control response is presented. The behavior of the open loop & closed loop controllers is studied in the presence and absence of an external disturbance. The external disturbance is considered to be a gradient terrain.

In the last section, the conclusion of the thesis is presented. Some useful hints are recommended to overcome the difficulties that the cruise control of the machine is faced.

Preface

I would like to thank Professor Kalevi Huhtala, the head of IHA department to provide an interesting topic as the master thesis. I would like to thank my thesis supervisors Dr. Reza Ghabcheloo and Dr. Mika Hyvönen for all their help and guidance. I would like to extend my gratitude to Joni Backas and Miika Ahopelto PhD. Students for helping me to do the thesis.

My thanks go to my Family Farah, Farnia and Ahmad for providing support through love and encouragement.

I would like to dedicate this thesis to my lovely grandpa (R.I.P)

Nima Rashvand

Tampere, 2012

Table of Contents

List of Tables

Lists of Figures

Nomenclature

A_f	$frontal\ area\ of\ the\ machine, m^2$
C_d	$dimensionless\ damping\ coefficient$
C_f	$internal\ friction\ coefficient,$
C_l	$hydraulic\ capacitance \frac{m^3}{Pa}$
C_d	$drag\ force\ coefficient$
F_f	$longitudinal\ tire\ force, N$
F_{aero}	$aerodynamic\ force$, N
F_{zr}	the normal force acting on tire, N
F_{fr}	the longitudinal tire force, N
g	$gravity\ acceleration, \frac{m}{s^2}$
GUI	graphical user interface
GIMsim	the simulator platform
HM	hydraulic motor
h	$the\ heigth\ of\ center\ mass, m$
HST	hydrostatic transmission
IMU	Inertial measurement unit
J_t	$moment\ of\ inertia, kgm^2$
K_{Tm}	$Total\ leakage\ coefficient\ of\ motor, \frac{m^3}{Pas}$
K_{im}	$motor\ internal\ leakage\ coefficient, \frac{m^3}{Pas}$
K_{em}	$motor\ external\ leakage\ coefficient$
K_t	$Laminar\ flow\ coefficient$

K_i	$Internal\ leakage\ coefficient, \frac{m^3}{Pas}$
K_e	$External\ leakage\ coefficient, \frac{m^3}{Pas}$
$K_{T(m+p)}$	Total leakage coefficient of pump and motor, $\frac{m^3}{Pas}$
$K_{e(m+P)}$	$motor\ and\ pump\ \ external\ leakage\ coefficient$
$K_{i(m+P)}$	$motor\ and\ pump\ internal\ leakage\ coefficient$
L	gradient Terrain Length, m
l_r	$rear\ axle\ length, m$
l_f	$front\ axle\ length, m$
M	$Mass\ of\ the\ machine, kg$
Q_{fr}	$flow\ to\ the\ front\ right\ motor, \frac{m^3}{s}$
Q_{fl}	$ideal\ flow\ to\ the\ front\ left\ motor, \frac{m^3}{s}$
Q_{rr}	$ideal\ flow\ to\ the\ rear\ right\ motor, \frac{m^3}{s}$
Q_{rl}	$ideal\ flow\ to\ the\ rear\ left\ motor, \frac{m^3}{s}$
Q_L	$total\ leakage\ flow, \frac{m^3}{s}$
Qs	$supplied\ flow, \frac{m^3}{s}$
Q_{im}	$motor\ internal\ leakage\ flow, \frac{m^3}{s}$
Q_{em}	$motor\ external\ leakage\ flow, \frac{m^3}{s}$
Q_{LT}	$Total\ leakage\ flow, \frac{m^3}{s}$

Q_{LM}	$motor\ leakage\ flow, \frac{m^3}{s}$
Q_{LP}	$pump\ leakage\ flow, \frac{m^3}{s}$
R_{fr}	$rolling\ resistance\ force, N$
r	$wheel\ radius, m$
T	$Torque\ out\ of\ the\ diesel\ Engine, Nm$
T_w	$Effective\ torque\ on\ the\ wheel, Nm$
T_g	$ideal\ generated\ torque, Nm$
T_d	$damping\ torque, Nm$
T_f	$friction\ torque, Nm$
T_c	$seal\ friction\ torque, Nm$
T_l	$delivered\ net\ torque, Nm$
V	$volume\ of\ high\ pressure\ line\ of\ HST\ circuit, m^3$
V_m	$volumetric\ displacement\ setting\ of\ a\ hydraulic\ motor$
V_p	$volumetric\ displacement\ setting\ of\ a\ hydraulic\ pump$
V_x	$velocity\ of\ the\ machine, \frac{m}{s}$
V_{wind}	$velocity\ of\ the\ wind, \frac{m}{s}$
$\ddot{x}$	$longitudinal\ acceleration\ of\ the\ machine, \frac{m}{s^2}$
α	$slop\ of\ the\ gradient\ surface$
β_t	$viscouse\ damping\ coefficient$
β	center link angle, rad
β_e	$effective\ bulk\ modulus, Pa$
$\dot{\theta_m}$	$motor\ rotational\ speed$, rad/s

$\dot{\theta_{rr}}$ $rotational\ speed\ of\ the\ rear\ right\ motor, \frac{rad}{s}$

$\dot{\theta_{rl}}$ $rotational\ speed\ of\ the\ rear\ left\ motor, \frac{rad}{s}$

$\ddot{\theta_{m}}$ $rotational\ acceleration\ of\ hydraulic\ motor, \frac{rad}{s^2}$

$\dot{\theta_{fr}}$ $rotational\ speed\ of\ the\ front\ right\ motor, \frac{rad}{s}$

$\dot{\theta_{fl}}$ $rotational\ speed\ of\ the\ front\ left\ motor, \frac{rad}{s}$

$\ddot{\theta_{fr}}$ $rotational\ acceleration\ of\ the\ front\ right\ wheel, \frac{rad}{s^2}$

η_{hmm} Mechanical efficiency of motor

η_{hmp} Mechanical efficiency of pump

η_{vm} Volumetric efficiency of motor

η_{vp} Volumetric efficiency of pump

η_{tp} overal pump efficiency

Δp $pressure\ difference\ between\ input\ and\ output\ ports\ of\ pump, Pa$

ε_p $displacement\ setting\ of\ hydraulic\ pump$

ε_m $displacement\ setting\ of\ hydraulic\ motor$

ω_p $Rotational\ velocity\ of\ the\ diesel\ engine, RPM$

μ $absolute\ viscosity\ of\ fluid$

ρ $Air\ Density \frac{kg}{m^3}$

1.0 Introduction

This thesis focuses on the dynamic modeling and cruise control of an autonomous mobile machine (wheel loader) with the hydrostatic transmission power train. In autonomous driving, the issue of speed control is very important because the machine should be able to follow the desired speed as precise as possible. In this thesis a feedback control methodology is designed for the machine to avoid tracking errors as much as possible and follows the desired speed. The loader is built in IHA department. The machine has one Diesel Engine as the main source of power, one main hydraulic pump which converts the mechanical power to hydraulic power and makes the fluid flow into the power transmission system and four hydraulic motors which convert the hydraulic power to mechanical power.

1.1 Background

To design the control methodology, a simplified model of the machine is needed to be defined. The calculated model will be compared with GIMsim to be validated and when we are talking about IHA machine's results, the results obtained in GIMsim is meant. GIMsim is the main simulator platform at IHA which allow us to test different models without using the real Machine. Tire-terrain interaction, body dynamics, diesel engine, hydrostatic transmission system, and sensor models are the elements which are modeled in the simulator. Components like hydraulic pumps, motors, control valve of the steering cylinder and pressure control valve are verified via laboratory measurements at IHA. The real time simulation model is distributed into five parallel PC's to enable effective simulation of the entire mobile machine. GIMsim is used to evaluate different type of hydraulic circuits, standard manufactures components, electronics, and low level control systems before building the real machine. PCs are connected through local area network. The figure 1 shows the architecture of the local network used in GIMsim.

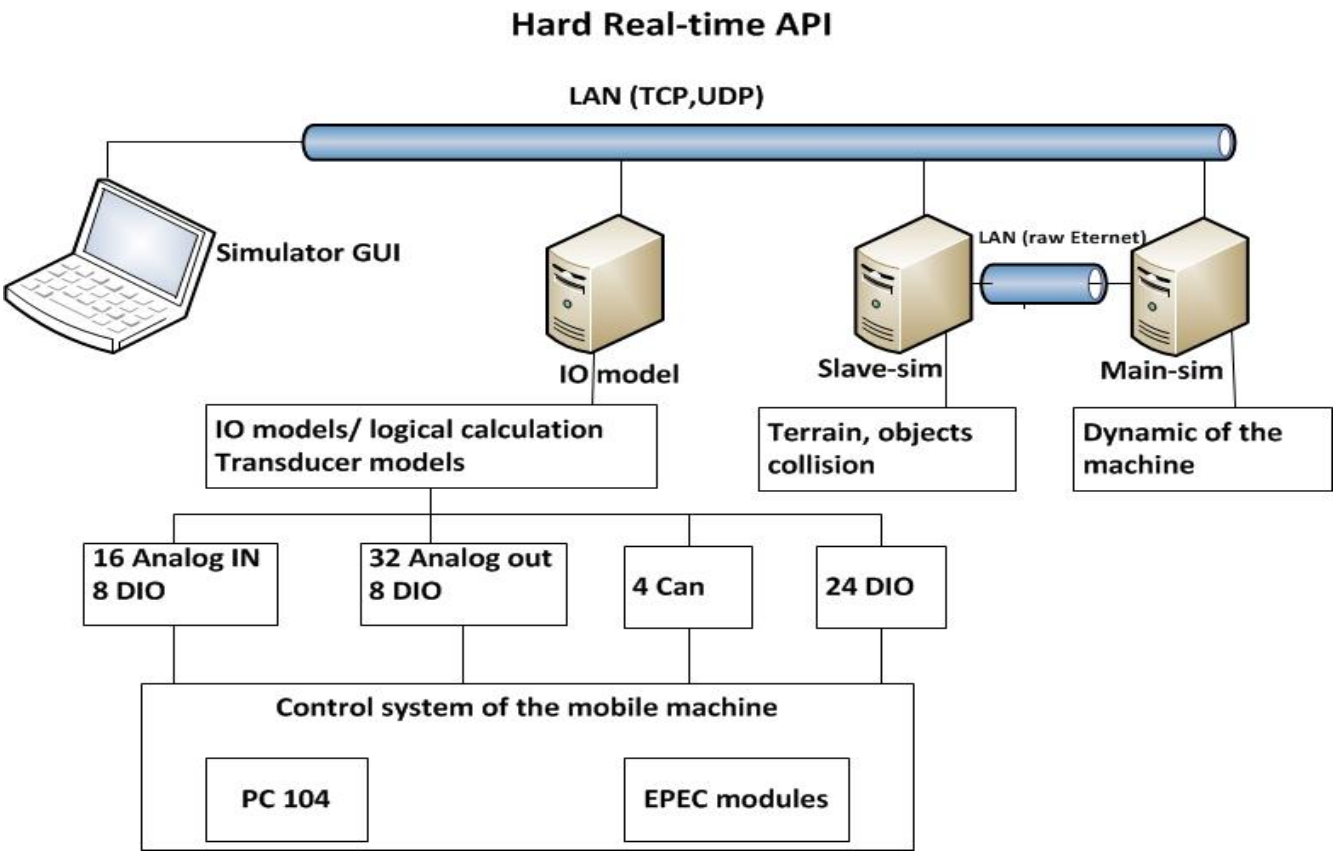

Figure 1: architecture of the network in Simulator

Graphical user interface (GUI) is an interface between human and computers. It allows the user to interact with the computers with Images rather than text commands. At the IHA's Simulator GUI interacts between the user and the system by visualizing the IHA Machine. The GUI visualizes the motion of the machine in real time and the user can see the performance of the machine in different situations. Also GUI lets the user to see the environment where the machine is moving. It is possible to change the physical characteristics of the environment via terrain selection option in the model. GUI not only visualizes the motion of the machine itself but also can visualize the motion of the booms which do the hydraulic works.

1.2 Objective

This thesis aims to investigate modeling and cruise control for articulated frame-steering mobile machine and implement a feedback control for cruise control. The objectives are summarized as:

. Study the hydrostatic power transmission

. Study the body dynamic of the machine

. Study the control methodology used in the system

. Compare the results with GIMsim's data

2.0 System overview

In this chapter, an overview about the dynamic model of the wheel loader and its hydraulic power transmission will be given. The intention of this chapter is to give the reader a better understanding of how a hydrostatic transmission works and why it is used in wheel loaders.

2.1 wheel loader (IHA machine)

The IHA machine which has been built in the department of intelligent hydraulics and automation at Tampere University of Technology is a wheel loader. The task of this vehicle is to pick up load and carrying it to the destination point autonomously. The focus of this thesis is to control the cruise of the vehicle and to avoid overshoot in the output in presence of measured & unmeasured disturbances. The vehicle has a diesel engine with maximum power 100 KW and is the only source of power to move the boom and vehicle itself. The power can be transmitted simultaneously to hydrostatic drive and work hydraulics/actuators. Set point for each power user (drive and work hydraulics) is defined by power management unit. The decision is for optimal fuel consumption for a given task. Optimal power management is not discussed here, see [2] for detail.

Figure 2: The wheel loader used in the GIM project (IHA machine)

The weight of the vehicle is nearly 4 Tons and it has one variable displacement hydraulic pump and four fixed displacement hydraulic motor.

The vehicle can be controlled in three modes: 1- Manual 2- teleoperate (remote) 3- Autonomous

The cruise control should be able to handle the task for all three driving modes.

2.2 Hydraulic Pump

The task of hydraulic pump is to convert the Engine mechanical power into fluid power. There is power loss in the process of converting power. The overall pump efficiency is defined as the useful output power divided by the supplied input power:

$$\eta_{tp} = \Delta p Q_s / T\omega_p \quad (2.1)$$

Where:

Δp *is the pressure difference between input and output ports of pump*, Pa

Qs *is supplied flow*, $\frac{m^3}{s}$

T *is Torque out of the diesel Engine*, Nm

ω_p *is Rotational velocity of the diesel engine*, RPM

The overall efficiency is the multiplication of hydro mechanical Efficiency and volumetric efficiency.

$$\eta_{tp} = \eta_{hmp} . \eta_{vp} \quad (2.2)$$

Where:

η_{hmp} Is hydro mechanical efficiency of pump

η_{vp} is Volumetric efficiency of pump

η_{tp} is overal pump efficiency

Mechanical efficiency is equal to:

$$\eta_{hmp} = V_p \Delta p / T \quad (2.3)$$

Where:

V_p *is volumetric displacement setting of a hydraulic pump*

Volumetric Efficiency is:

$$\eta_{vp} = \frac{Q_s}{\varepsilon_p . V_p . \omega_p} \quad (2.4)$$

A method is provided by the variable displacement pumps for the direct control of a hydraulic actuator without the use of an intermediate valve. Displacement controlled pumps improve the efficiency of the system, because the intermediate valves are always energy drain on hydraulic control systems.

In hydraulic machines, Leakage flows and friction are the source of losses. There are two types of leakage flow. Internal or cross-port leakage between the lines and external leakage from each motor and pump chamber past the pistons to case drain. The leakage flows are laminar and, therefore, they are proportional to the first power of pressure. The reason of laminar flow is that all mating clearances in a pump and motor are intentionally made small to reduce losses. The overall leakage is proportional to pressure difference and may be written:

$$Q_L = K_t . \Delta p \quad (2.5)$$

Where:

Q_L *is total leakage flow,* $\frac{m^3}{s}$

K_t *is Laminar flow coefficient*

2.3 Hydraulic motors

There are two types of actuators 1: linear actuator 2: rotary actuator. Rotational output for hydraulic control systems can be generated by rotary actuators. Pumps converts rotating shaft power into fluid power, rotary actuators do just the opposite. They convert fluid power into rotary shaft power. There are two types of rotary actuators constant and variable displacement. The hydraulic motor which is used in the power transmission unit is a constant one with two fixed (1&1/2) volumetric displacement.

There are at least three sources of torque losses which detract from the generated torque: [15]

1. A torque proportional to motor speed exists because torque is required to shear the fluid in the small clearance between mechanical elements in relative motion. This damping torque can be written as

$$T_d = \beta_t . \dot{\theta_m} = C_d . V_m . \mu . \dot{\theta_m} \quad (2.6)$$

Where:

T_d *is damping torque*, Nm

β_t *is viscouse damping coefficient*

V_m *is volumetric displacement setting of a hydraulic motor*

C_d *is dimensionless damping coefficient*

μ *is absolute viscosity of fluid*

$\dot{\theta_m}$ *is motor rotational speed, rad/s*

2. In piston motors some sort of lever mechanism is required to translate piston motion into rotary shaft motion. An examination of the forces on each piston will show a friction force opposing motion of the piston in its bore that is proportional to the pressure acting on the piston area.

$$T_f = C_f . V_m . \Delta p \tag{2.7}$$

Where:

T_f *is friction torque*, Nm

C_f *is internal friction coefficient*

3. There is also a small torque required to overcome seal friction that is constant but reverses direction with speed. This torque will be denoted
T_c *but can be neglected altogether in most instances*.

The net torque delivered to the load is:

$$T_l = V_m . \Delta p - C_d . V_m . \mu . \dot{\theta_m} - C_f . V_m . \Delta p - T_c \tag{2.8}$$

Where:

T_l *is delivered net torque*, Nm

T_c *is seal friction torque*, Nm

The volumetric efficiency is defined as the ratio of flow which results in motor speed (the ideal flow) to the flow supplied to the motor. Therefore according to the definition

$$\eta_{\mathrm{vm}} \equiv \frac{\varepsilon_m . V_m . \dot{\theta}_m}{Qs} \tag{2.9}$$

The mechanical efficiency is defined as the ratio of actual to ideal torque delivered by the motor:

$$\eta_{\mathrm{hmm}} \equiv \frac{T_l}{\varepsilon_m . V_m . \Delta p} \tag{2.10}$$

2.4 Volumetric efficiency

The volumetric efficiency is defined as the ratio of flow which results in motor speed (the ideal flow) to the flow supplied to the motor. Therefore by definition:

$$\eta_{\mathrm{vm}} \equiv \frac{\varepsilon_m . V_m . \dot{\theta_m}}{Qs}$$

The volumetric efficiency of the hydraulic motor with full displacement has been shown in the Table 1:

Table 1: The volumetric efficiency of motor with full displacement

Motor speed (RPM) / Pressure (bar)	0	25	50	100
20	0.9	0.97	0.9874	0.98
100	0.85	0.9489	0.9744	0.9872
200	0.81	0.9148	0.9574	0.9787
300	0.77	0.8723	0.9361	0.9680
400	0.75	0.8297	0.9148	0.9581

The data of volumetric efficiency is measured for the pressure below 300 bars and it is estimated for the pressure higher than 300 bars & motor speed around 0 rpm. The same data is shown in the Figure 3. The volumetric efficiency is depended on differential pressure and motor angular speed.

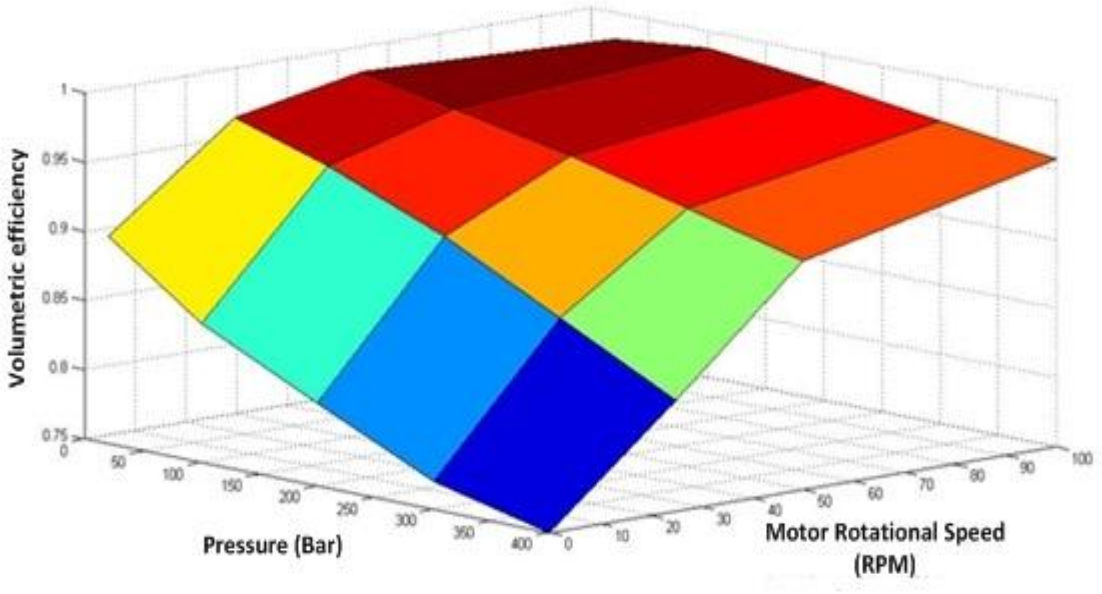

Figure 3: The volumetric efficiency of motor

The volumetric efficiency of the hydraulic pump has been shown in the table 2:

Table 2: The volumetric efficiency of the pump at 1200 rpm

Pump displacement / Pressure (bar)	~ 0 %	30%	60%	100%
20	0.4	0.9	0.95	0.97
100	0.3	0.5868	0.7581	0.8661
200	0.2	0.3658	0.6422	0.8007
300	0.1	0.1689	0.5001	0.7304
400	0.05	0.0901	0.45	0.6401

The data of volumetric efficiency is measured for the pressure below 300 bars and it is estimated for the pressure higher than 300 bars & pump displacement around 0%. The same data is shown in the figure 4. The volumetric efficiency is depended on pump displacement and differential pressure. The diesel engine rpm is kept constant at 1200 rpm.

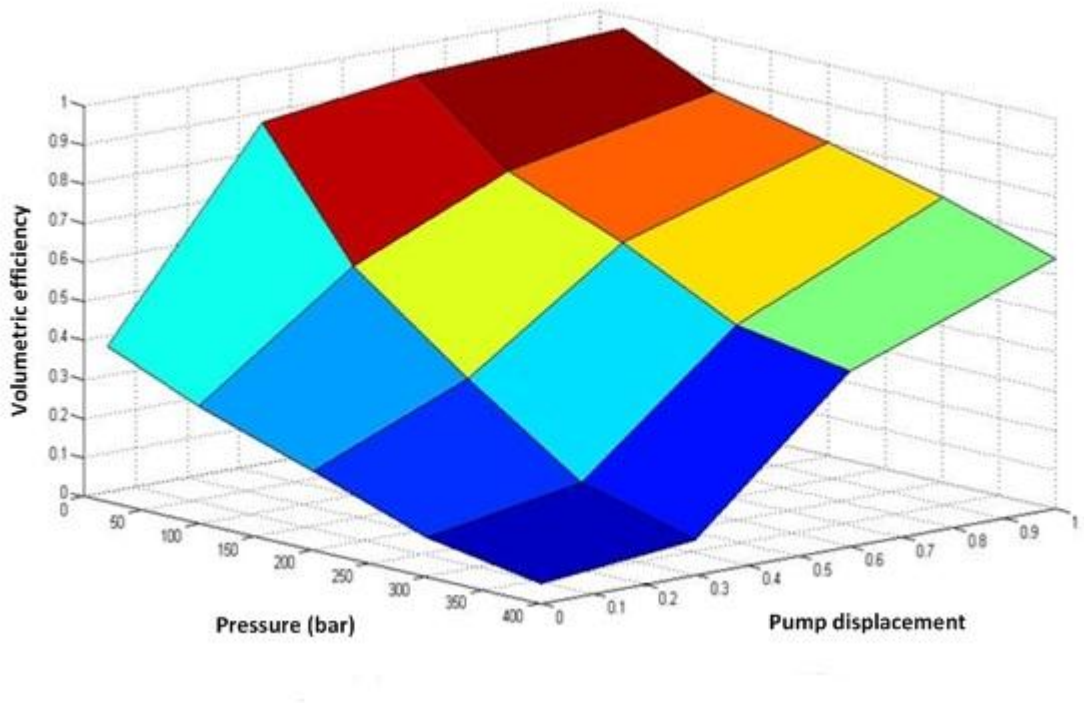

Figure 4: the volumetric efficiency of Pump

2.5 Hydro mechanical efficiency

According to Merritt, H [15]'' there are at least three source of torque losses which detract from the ideal generated torque''.

The ideal generated torque is:

$$T_g = V_m(\Delta p) \tag{2.11}$$

The hydro mechanical efficiency can be defined as the ratio of actual to ideal torque delivered by the motor.

$$\eta_{\mathrm{hmm}} \equiv \frac{\mathrm{T_l}}{\varepsilon_m . V_m . \Delta p}$$

The hydro mechanical efficiency of motor with full displacement has been shown in the Table 3.

Table 3: The hydro mechanical efficiency of motor with full displacement

Motor speed (RPM) / Pressure (bar)	0	25	50	100
20	0.48	0.81	0.85	0.86
100	0.52	0.83	0.89	0.885
200	0.60	0.85	0.9	0.9207
300	0.64	0.87	0.92	0.9238
400	0.68	0.88	0.91	0.92

The data of hydro mechanical efficiency is measured for the pressure below 300 bars and it is estimated for the pressure higher than 300 bars & motor speed around 0 rpm. The same data is shown in the figure 5. The hydro mechanical efficiency of the motor is depended on angular velocity and differential pressure over motor.

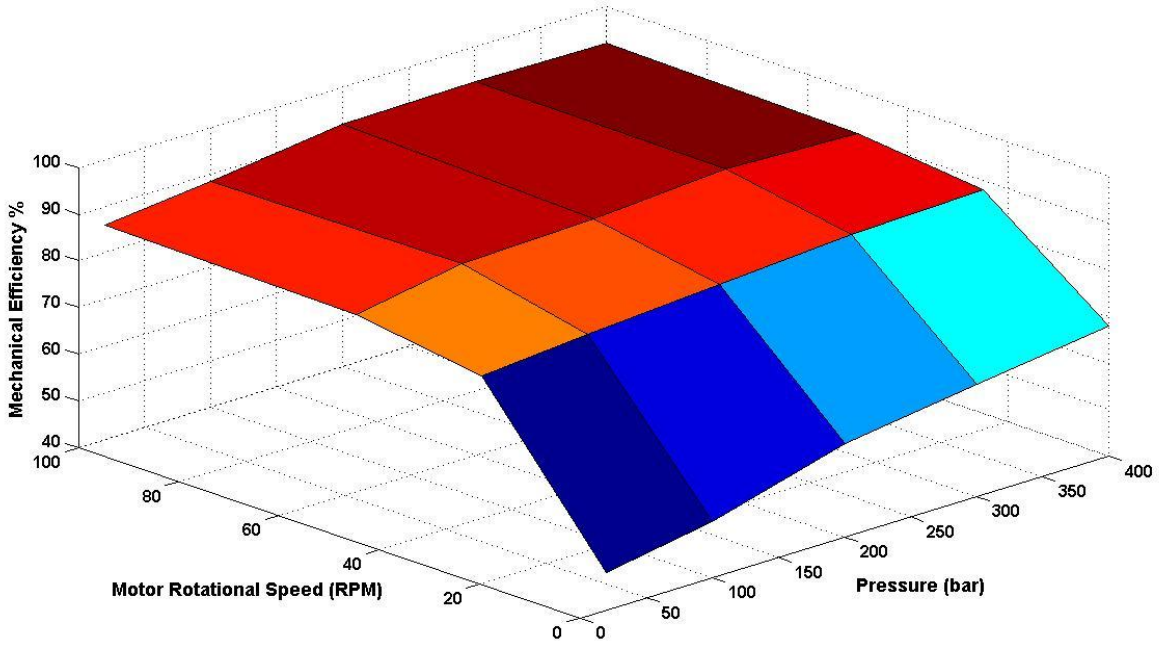

Figure 5: the hydro mechanical efficiency of the motor

2.6 Leakage Losses

According to Merritt, H [15], ‘’there are two sources of losses in hydraulic machines which are leakage flows and friction’’. Figure 6 demonstrates an axial piston motor which has a stationary wobble and has the ability to convert piston motion into rotary motion. This motor utilizes the valve plate porting mechanism. One of the characteristics of the mechanism is that the leakage & friction losses of all pistons are lumped. Also, Figure 6, shows that there are two types of leakage flow within the mechanism: Internal or cross-port leakage which functions between the lines and also the external leakage from each motor chamber which is located past the pistons to case drain. In order to reduce losses, the mating clearances in a motor or a pump are intentionally made small. This phenomenon results in a fact that the leakage flows will become laminar and consequently they will be proportional to the first power of pressure.

The internal leakage is proportional to motor pressure difference and may be written

$$Q_{im} = K_{im}\Delta p \tag{2.12}$$

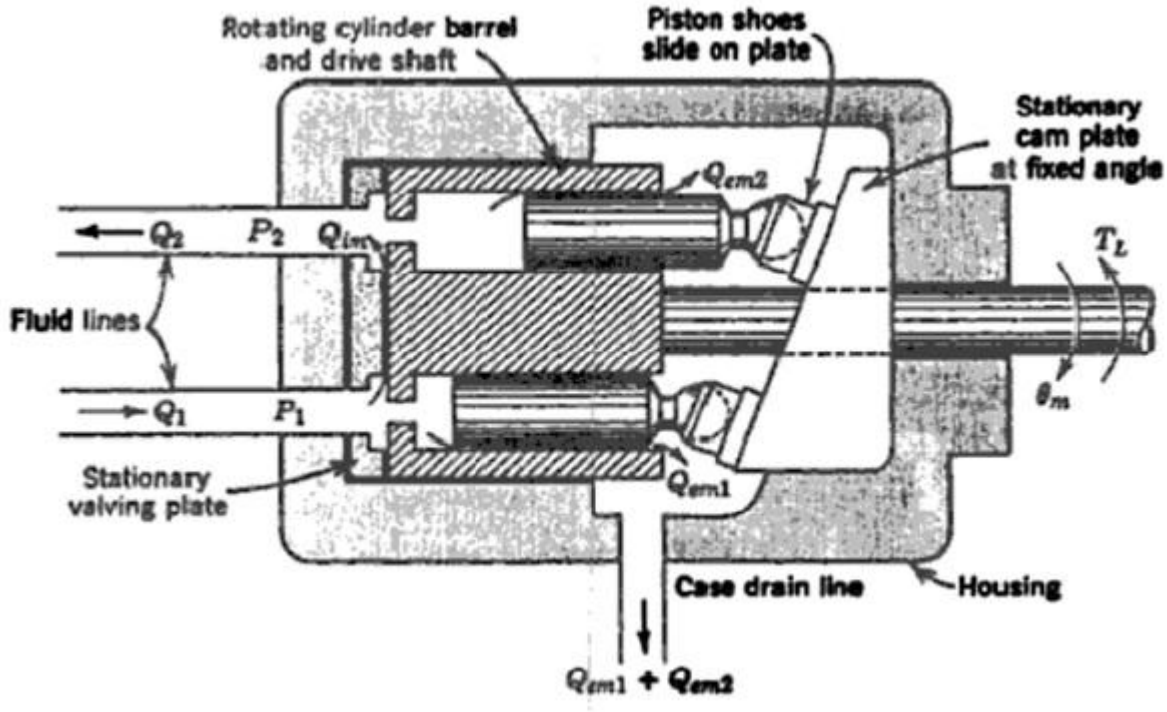

Figure 6: Schematic diagram of a fixed displacement axial piston motor

K_{im} is internal leakage coefficient and P_L is pressure difference across motor. The external leakage in each chamber is proportional to the particular chamber pressure (assuming negligible drain pressure) and may be written

$$Q_{em} = K_{em}\Delta p \tag{2.13}$$

K_{em} is the motor external leakage coefficient. The total leakage flow of motor can be defined as

$$Q_l = (K_{em} + K_{im}).\Delta p \tag{2.14}$$

The sum of internal and external leakages of motor can be shown by:

$$K_{Tm} = K_{em} + K_{im}$$

Another source of flow losses in hydraulic machines is oil compressibility which is depended on oil bulk modulus and the volumetric compressibility can be defined by the following equation:

$$\Delta V = \frac{V_0}{\beta_e}.\frac{d(\Delta p)}{dt} \tag{2.15}$$

Where

V_0 is $the\ volume\ of\ high\ pressure\ line\ of\ HST\ circuit, m^3$

β_e is the oil effective bulk modulus, MPa

$\frac{V_0}{\beta_e} = C_l$ which is the hydraulic capacitance in the equations and is equal with (5×10^{-12}), $\frac{m^3}{Pa}$.

Total leakage flow of pump and motors:

As the equation (2.5 & 2.14) illustrates the total leakage flow is depended on the Leakage coefficient and differential pressure over pump and motor. Because there are 4 motor and one pump the total leakage coefficient can be derived from

$$K_{T(m+P)} = K_{e(m+P)} + K_{i(m+P)} \tag{2.16}$$

The leakage flow of the pump can be calculated with

$$Q_{LP} = \varepsilon_P V_P \omega_P (1 - \eta_{\mathrm{vp}}) \tag{2.17}$$

And also the leakage flow of motor can be calculated with

$$Q_{Lm} = \varepsilon_m V_m \dot{\theta}_m \left(\frac{1-\eta_{\mathrm{vm}}}{\eta_{\mathrm{vm}}}\right) \tag{2.18}$$

And finally the total leakage flow of pump and 4 parallel motors can be obtained by

$$Q_{LT} = Q_{LM} + Q_{LP} \tag{2.19}$$

The relation between total leakage coefficient and total leakage flow can be found with

$$Q_{LT} = K_{T(m+P)}.\Delta p \tag{2.20}$$

The total leakage coefficient of pump and motors is shown in the figure 7. The pump displacement setting changes between 0-1 and the engine rotational speed changes between 1000-2200 rpm. When the motor rotational speed goes to zero the leakage coefficient also goes to zero and it means that the leakage flow stops when the vehicle is stopped.

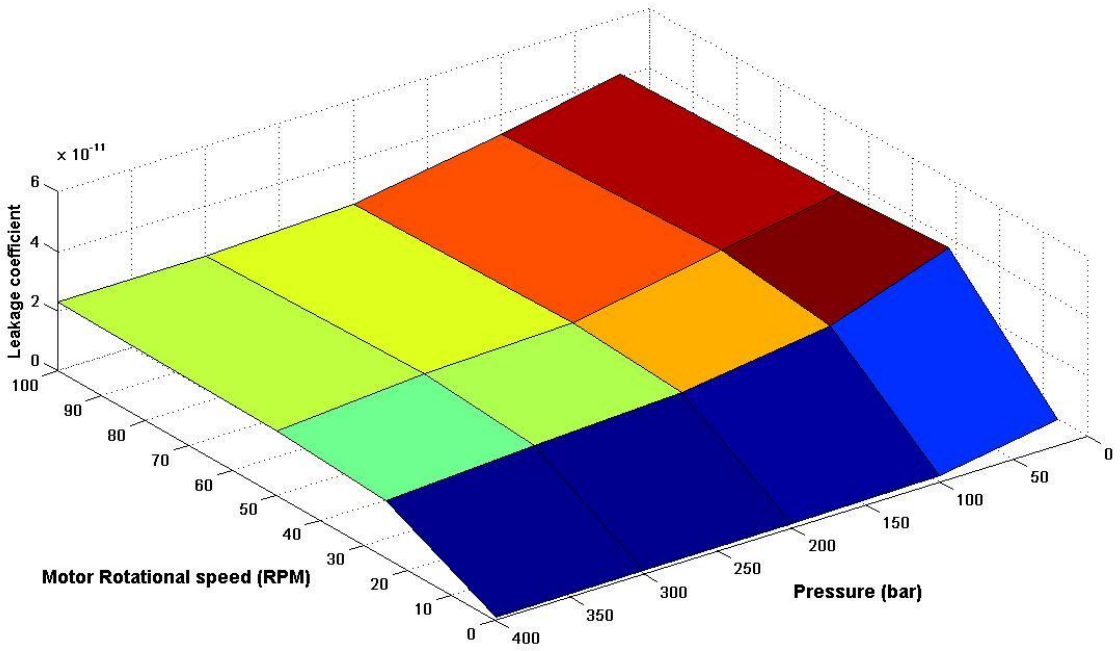

Figure 7: The total leakage coefficient of pump and motors

The total leakage flow is shown in the figure 8, as it shows the total leakage is depended on the pressure over pump and motor angular speed (rpm).

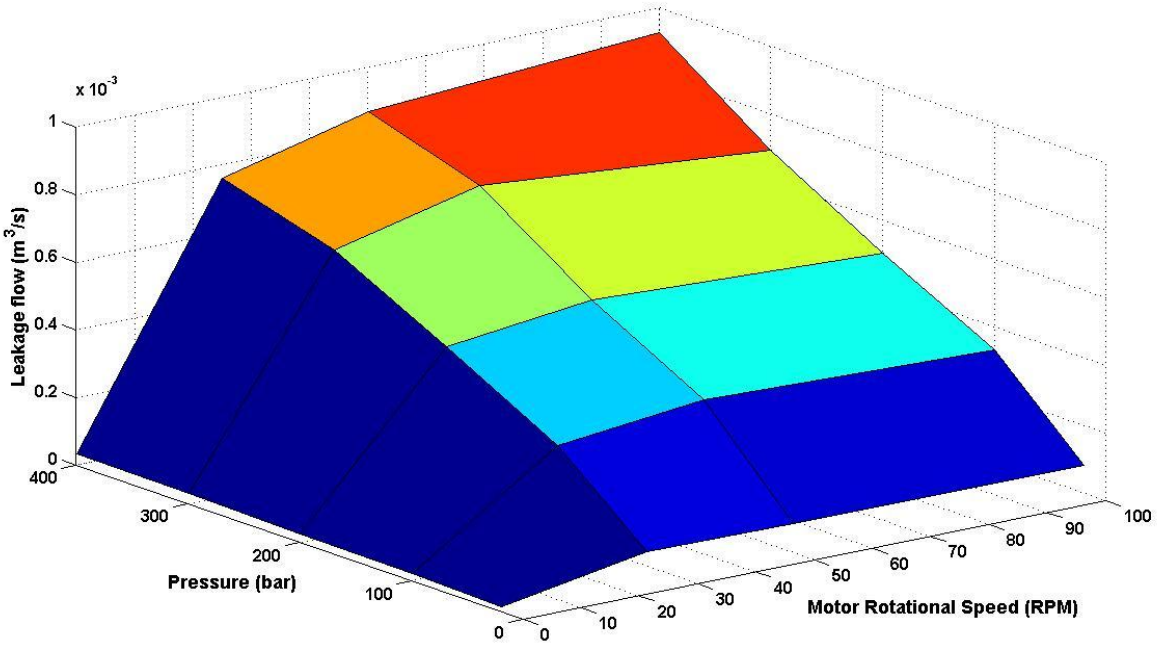

Figure 8: the total leakage flow

2.7 Diesel Engine

The task of the diesel engine is to convert the chemical energy of fuel into rotating mechanical energy of the shaft. The shaft is connected to the hydraulic pumps. The diesel engine of the IHA wheel loader is capable to produce maximum 100 KW power and the maximum rotational velocity of the engine is 2200 rpm. As the power curve figure 9 shows the maximum power happens around 2000 rpm of the engine's rotational velocity. The lowest diesel engine rotational velocity is considered to be 1000 rpm.

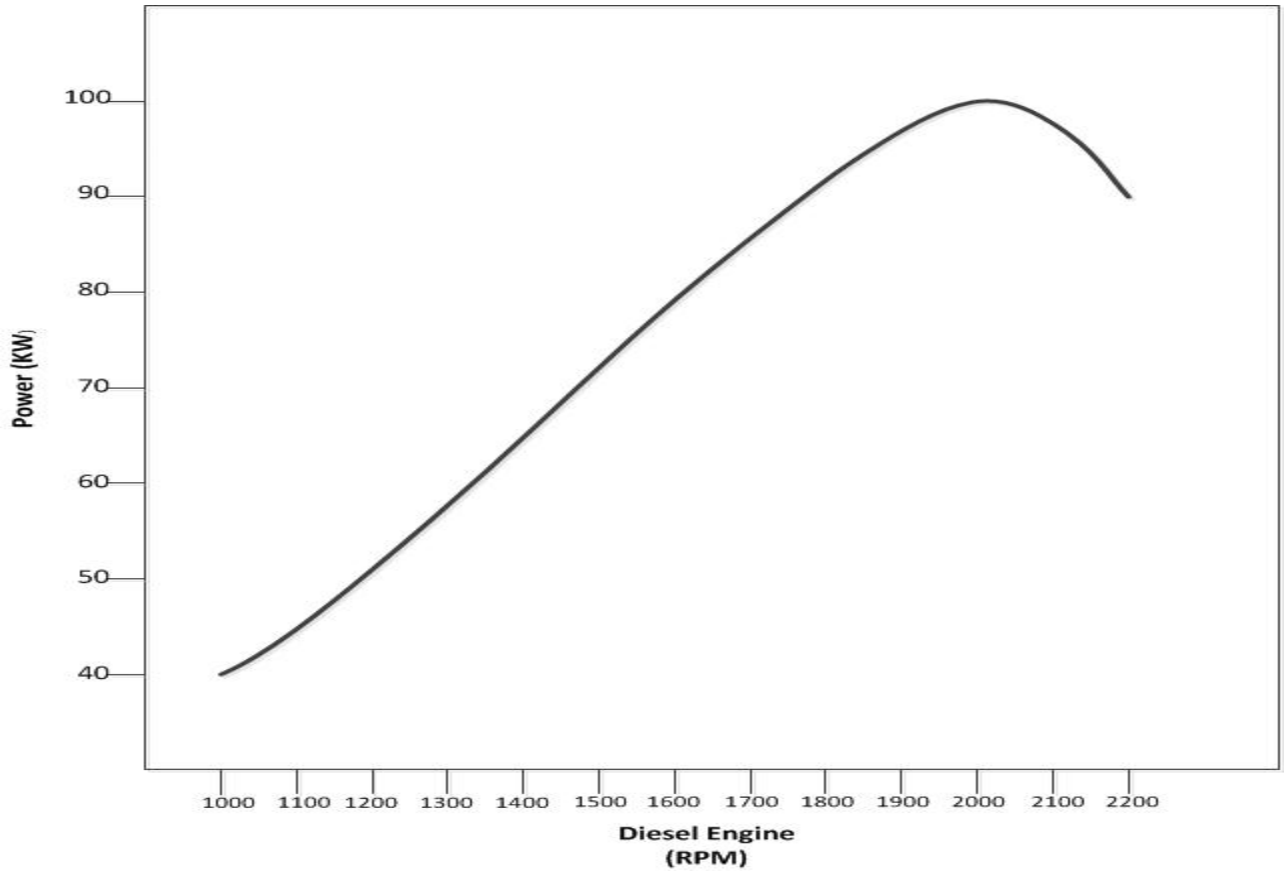

Figure 9: Diesel engine power curve

2.8 Power transmission line

Any Hydraulic motor used in combination with various pumps is termed as hydrostatic drives [4]. Hydrostatic drive can be classified based on torque range requirement. There are 2 types of hydrostatic drive: 1-open loop 2-closed loop.

1. Open loop

An open loop hydrostatic drive has the motor inlet connected to the pump outlet and the motor outlet connected to the reservoir. The rotational speed of the motor depends on pump flow rate and motor displacement.

2. Closed loop

A closed loop hydrostatic drive has motor inlet connected to pump outlet and motor outlet connected to pump inlet. The closed loop figure 10 shows motor rotation in both directions with variable pump input which will vary motor speed and direction. Any leakage in the system is made up by the replenishing pump.

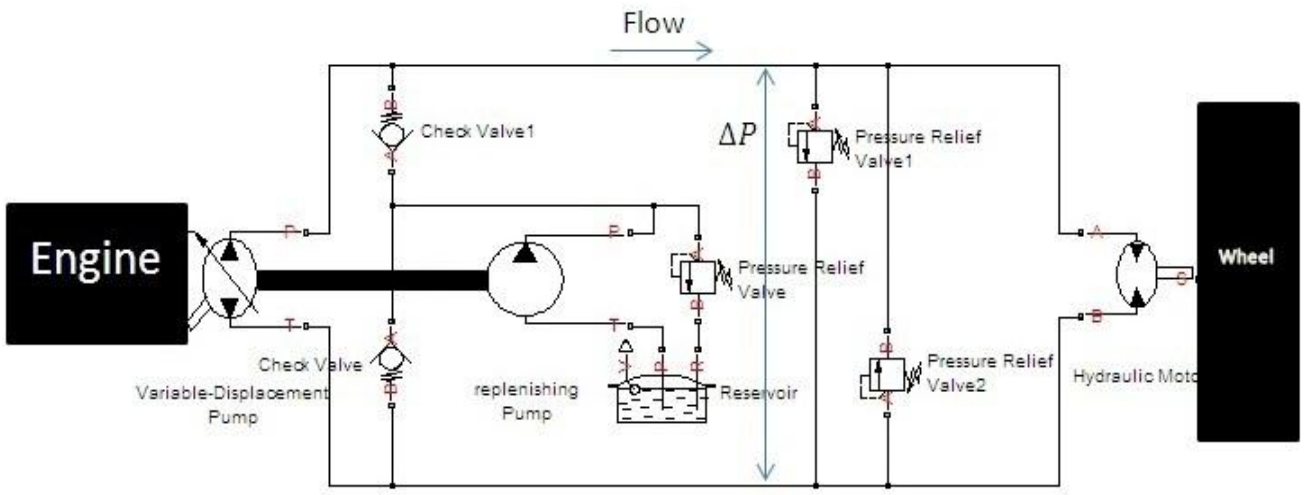

Figure 10: Closed loop with one Hydraulic Motor

The configuration of hydrostatic transmission drive in IHA machine is closed loop and parallel. In IHA machine motors are connected in parallel. The outlet of the pump is connected to all four motors delivering the same pressure to all the motors at the same time. Since all motors receive the same pressure, the maximum pressure at any time is determined by the drive wheel that has the least amount of rolling resistance. In a curved trajectory while the vehicle is in a turning condition the outer set of wheels will track faster than the inner set.

On a curved trajectory, speeds of the wheels (equivalently the flows to the HMs) will not be equal. Parallel configuration may function in many cases, but total traction force will be lost if one tire loses traction since the HMs are in parallel and have the same pressure. This happens when the connection between the terrain and one tire is lost. In this situation all the flows will cross the motor which has the Minimum traction force with terrain. In this condition the vehicle stops. This is one of the disadvantages of the Parallel configuration.

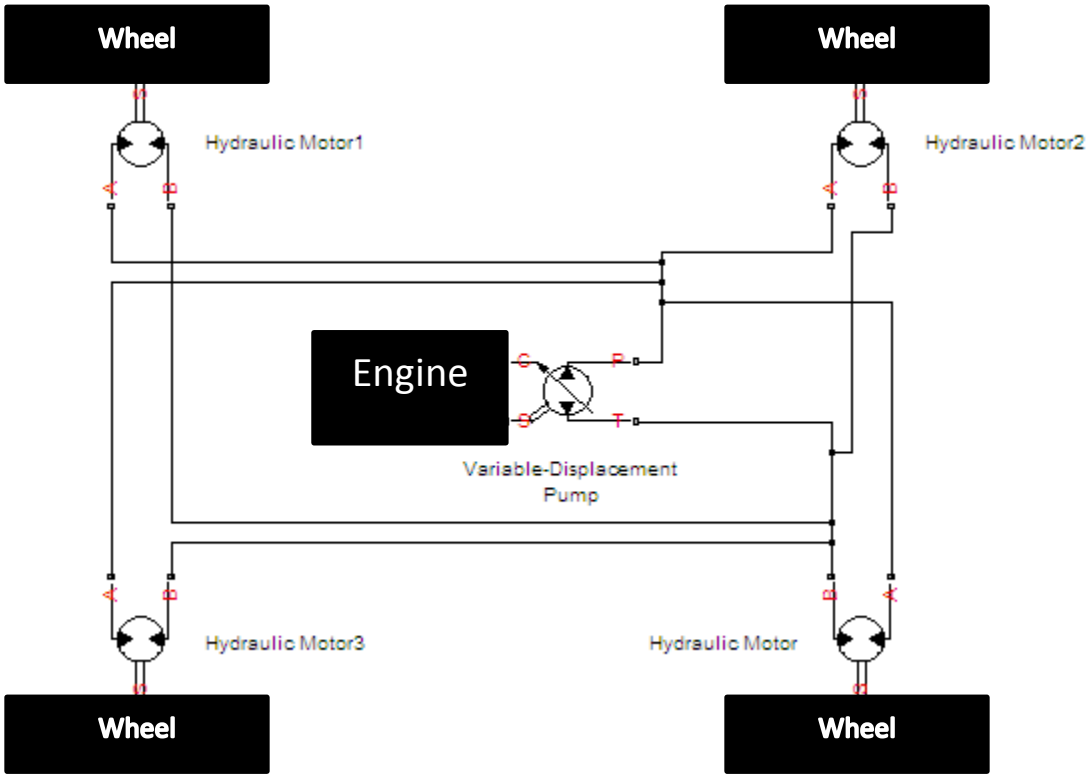

Figure 11: Parallel Hydrostatic transmission

2.9 simplified Vehicle model

To simplify the model, the vehicle is considered to have only one wheel and the volume displacement of the motor is four times bigger than the real one.

The dynamic model of the vehicle with one wheel is shown below, the model is derived under two simplifying assumption on tire-terrain interaction [8].

Assumption 1: there is no side-slips (no skidding).

Assumption 2: there is no slipping, that is, the ground speed of the contact points of the tire are equal to the rotational speeds of the tire multiplied by the tire radius.

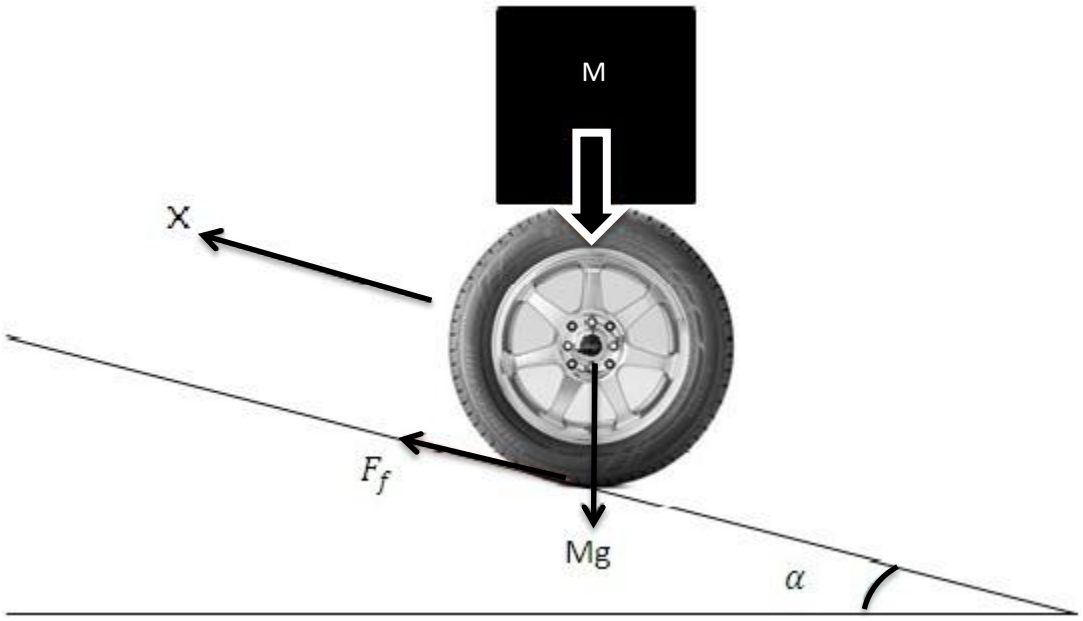

Figure 12: the simplified vehicle model

According to the figure 12 the dynamic model equation can be written:

$$F_f = M.\ddot{x} + M.g.sin(\alpha) \quad (2.21)$$

Where:

F_f *is the longitudinal tire force*

M *is the Mass of machine*

g *is the gravity acceleration*

α *is the slop of gradient surface*

The acting forces on the wheel can be described by the wheel's dynamic equation:

$$\sum T = J_t.\ddot{\theta_m} \quad (2.22)$$

Where:

$\sum T$ is the total torque on the wheel, Nm

J_t is the wheel's moment of inertia, kgm^2

$\ddot{\theta_m}$is the rotational acceleration of the motor, $\frac{rad}{s^2}$

By using the equations (2.4) & (2.9) & (2.10) & (2.14) & (2.15) & (2.21) & (2.22) the equation related to one pump and one motor can be written:

$$\frac{\varepsilon_p V_p \omega_p \eta_{\mathrm{vp}}}{C_l} - \frac{4\varepsilon_m V_m \dot{\theta_m}}{C_l} - \frac{K_{Tm}\Delta p}{C_l} = \frac{d\Delta p}{dt} \tag{2.23}$$

$$4\varepsilon_m V_m \Delta p\, \eta_{\mathrm{hmm}} - M.g.r.sin(\alpha) = (J_t + Mr^2).\ddot{\theta}_m \tag{2.24}$$

Where:

ω_p *is the Rotational velocity of the diesel engine*

ε_p *is the displacement setting of hydraulic pump*

C_l *is the hydraulic capacitance*

V_p *is the volumetric displacement of the big hydraulic pump*

ε_m *is the displacement setting of hydraulic motor*

K_{Tm} *is the total (internal and external) leakage coefficient of motor*

Δp *is the pressure difference over the main pump*

η_{hmm} is the hydro mechanical efficiency of motor

V_m *is the volumetric displacement of one hydraulic motor*

r *is the wheel radius*

Then the state space model is given by:

$$\begin{bmatrix} \dot{\Delta p} \\ \ddot{\theta_m} \end{bmatrix} = \begin{bmatrix} -K_{Tm}/C_l & -4\varepsilon_m V_m/C_l \\ 4\varepsilon_m V_m \eta_{\mathrm{hmm}}/J_t + Mr^2 & 0 \end{bmatrix} \begin{bmatrix} \Delta p \\ \dot{\theta_m} \end{bmatrix} + \begin{bmatrix} V_p \omega_p \eta_{\mathrm{vp}}/C_l & 0 \\ 0 & -M.g.r/J_t + Mr^2 \end{bmatrix} \begin{bmatrix} \varepsilon_p \\ \alpha \end{bmatrix}$$

$$\dot{X} = [0 \quad r] \begin{bmatrix} \Delta p \\ \dot{\theta_m} \end{bmatrix}$$

$\dot{X}$ is the output linear speed of the vehicle, m/s

Using small angle approximation $-20^{\circ} < \alpha < 20^{\circ}$ $\sin\alpha \cong \alpha$

2.10 Elaborated dynamic model of the machine consider more detail phenomenon

In this section the kinematics of the machine & hydraulic dynamics of the power transmission is studied.

2.10.1 Kinematics

In [8] Ghabcheloo et al discussed the problem with 2 simplification assumptions which were taken into consideration.

Assumption 1: there is no side-slips (no skidding) that the velocity vector of the unit is orthogonal to the axle. Assumption 2: there is no slipping, that is, the ground speed of the contact points of the tires are equal to the rotational speeds of the tires multiplied by the tire radius.

Attach a body-fixed frame to each unit indexed by i, where i stands for f and r, front and rear units, respectively. Based on the diagram in figure 13, kinematics equations of unit i under assumption are governed by

$$\begin{aligned} \dot{x_i} &= v_i cos\Psi_i \\ \dot{y_i} &= v_i sin\Psi_i \\ \dot{\Psi} &= \omega_i \end{aligned} \tag{2.25}$$

Where (x_i, y_i) denotes the coordinates of Q_i, the mid-point of the axles, and Ψ_i is the heading of unit i, Further, $v_i and\ \omega_i$ denote linear and angular speeds, respectively the inertial frame is called B and body-fixed frame is expressed by I, see for example figure 13. The center link angle (the angle between vectors (O$Q_f and\ Q_r O$) is then given by:

$$\beta = \Psi_f - \Psi_r \tag{2.26}$$

In the Figure 13, $|Q_r O|$ =l_r and $\left|OQ_f\right| = l_f$, where |.| denotes the Euclidian norm, d is distance

Between the effective contact points of the tires (length of axle), and 2r is the effective diameter

of the tires. We let ω_r and ω_l denote rotational speeds of right and left tires, respectively, of

Unit I in {f,r}, that is front and rear .

Under Assumption 1, the following kinematics constraints hold

$$v_r = v_f cos\beta + l_f \omega_f sin\beta \quad (2.27)$$

$$l_r \omega_r = -l_f \omega_f cos\beta + v_f sin\beta \quad (2.28)$$

$$\omega_f = \frac{l_r \dot{\beta} + v_f sin\beta}{l_f cos\beta + l_r} \quad (2.29)$$

Articulation velocity is the difference of rotational velocity between the front and rear units.

$$\omega_f - \omega_r = \dot{\beta} \quad (2.30)$$

The linear velocity of the front axle is:

$$v_f = \frac{r(\dot{\theta_{fr}} + \dot{\theta_{fl}})}{2} \quad (2.31)$$

Where:

$\dot{\theta_{fr}}$ *is the rotational velocity of the front right motor*
$\dot{\theta_{fl}}$ *is the rotational velocity of the front left motor*

The linear velocity of the rear axle is:

$$v_r = \frac{r(\dot{\theta_{rr}} + \dot{\theta_{rl}})}{2} \quad (2.32)$$

Where:

$\dot{\theta_{rr}}$ *is the rotational velocity of the rear right motor*

$\dot{\theta_{rl}}$ *is the rotational velocity of the rear left motor*

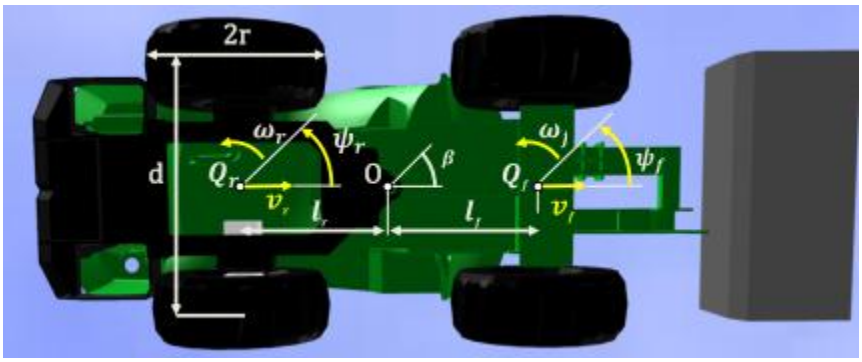

Figure 13: Body-fixed frames attached to a GIM mobile machine

If the rear axle velocity be written according to the front axle velocity, such a relation can be obtained:

$$v_r = v_f \left(\frac{1+cos\beta\frac{l_r}{l_f}}{cos\beta+\frac{l_r}{l_f}} \right) + \frac{l_r\dot{\beta}sin\beta}{cos\beta+\frac{l_r}{l_f}} \tag{2.33}$$

2.10.2 The flow division in power transmission line

Since the HMs are in parallel and have the same pressure it is assumed that the tires don't lose the traction force on the terrain. According to the figure 14 the effective flow which is coming from the pump will be divided between four HMs and by considering the leakage flow and also compressibility of the fluid this equation can be derived:

$$Q_s - Q_{fr} - Q_{fl} - Q_{rr} - Q_{rl} - K_{Tm}.\Delta p = C_l \frac{d\Delta p}{dt} \tag{2.34}$$

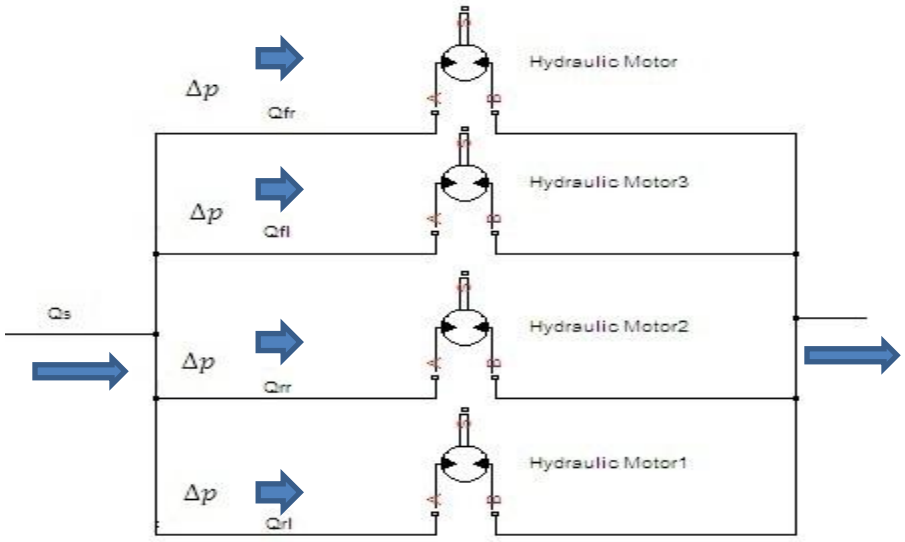

Figure 14: The flow division among HMs

As shown in the figure 14 in parallel configuration the pressure Δp over all four HMs is equal.

Where Qs is the pump supplied effective flow and K_{Tm} is the coefficient of internal and external leakage for motors which is a function of pressure in the system.

$$K_{Tm} = (K_{im} + K_{em}) \tag{2.35}$$

$$C_l = \frac{V_0}{\beta_e} \tag{2.36}$$

Where:

K_{em} *is the external leakage coefficient of motor*

K_{im} *is the internal leakage coefficient of motor*

K_{Tm} *is the total (internal and external) leakage coefficient of motor*

V_0 *is the volume of high pressure line of HST circuit*

β_e *is the effective bulk modulus*

C_l *is the hydraulic capacitance*

The effective flow from the pump:

$$Q_s = \eta_{\mathrm{vp}} \varepsilon_p \omega_p V_p \tag{2.37}$$

If we substitute (2.34) with (2.9) & (2.37) then:

$$\frac{\varepsilon_p \omega_p \eta_{\mathrm{vp}} V_p}{C_l} - \frac{4.\dot{\theta_{fr}}.V_m.\varepsilon_m}{C_l} - \frac{K_{Tm}}{C_l}\Delta p = \frac{d\Delta p}{dt} \tag{2.38}$$

$\dot{\theta_{fr}}$ is the rotational velocity of the front-right motor. The vehicle is supposed to move in a straight direction and flow division is equal between HMs.

2.11 Vehicle Longitudinal dynamic

Considering a vehicle moving on an inclined road as shown in the figure 15, there are different external longitudinal forces acting on the vehicle like aerodynamic drag forces, gravitational forces, and longitudinal tire forces and rolling resistance forces.

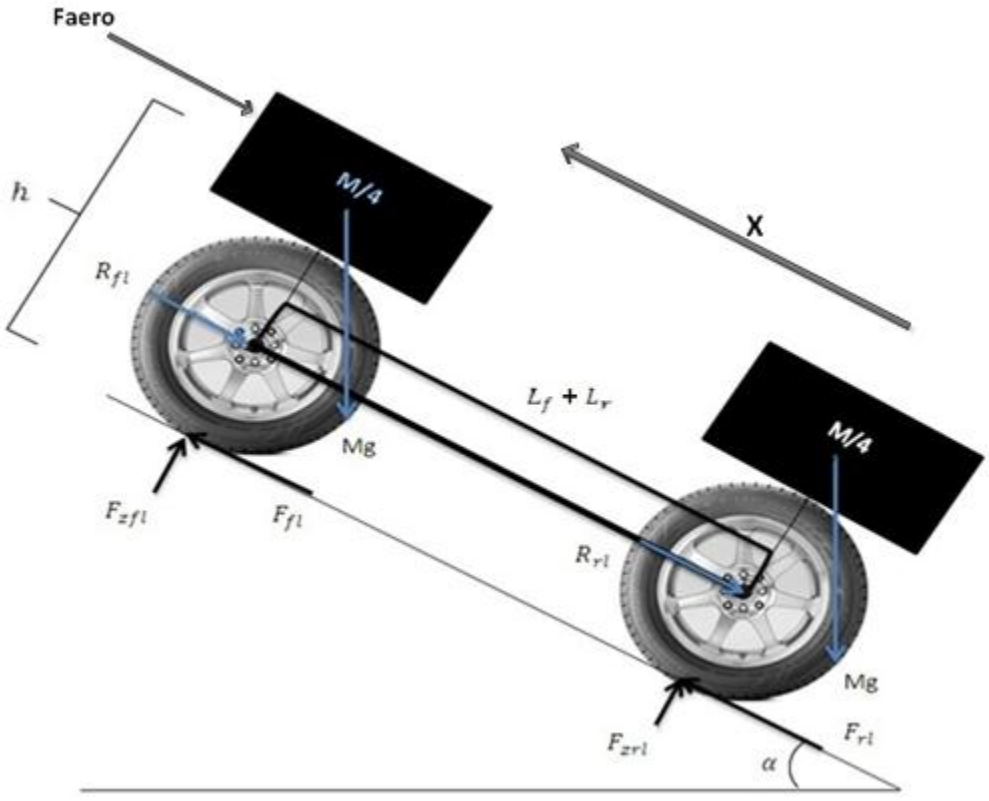

Figure 15: Longitudinal forces actin on a vehicle moving on an inclined road

In this section a review will be done on the external forces and their effect on the dynamic of the IHA machine. Because there are 4 HMs used in the drive-line, the effect of external longitudinal forces will be studied on each wheel. We assume that each HM moves ¼ total weight of the machine.

2.11.1 Aerodynamic drag force

The equivalent aerodynamic drag force on a vehicle can be represented as:

$$F_{aero} = \frac{1}{2}\rho C_d A_f (V_x + V_{wind})^2 \quad (2.39)$$

The aerodynamic drag force is proportional to the speed of the machine and because the application IHA machine as a wheel loader is not supposed to move with high speed the effect of this force on the dynamic of the machine can be neglected.

2.11.2 The longitudinal tire force

The friction forces from the ground that act on the tire can be described as ‘’longitudinal tire forces’’ [18].

According to experiments, longitudinal tire forces which are generated by each tire depend on the following factors:

a) The slip ratio
b) A portion of the vehicle weight which acts as the normal load on the tire
c) The friction coefficient between the tire & the road
d) is influenced by fore-aft location of the Center of gravity, vehicle longitudinal acceleration, aerodynamic drag forces and grade of the road.

According to the assumption 1 there is no sliding and skidding between the tire and ground. Therefore the slip ratio can be considered to be equal with 0.1 which has the highest tire force according to the figure 16.

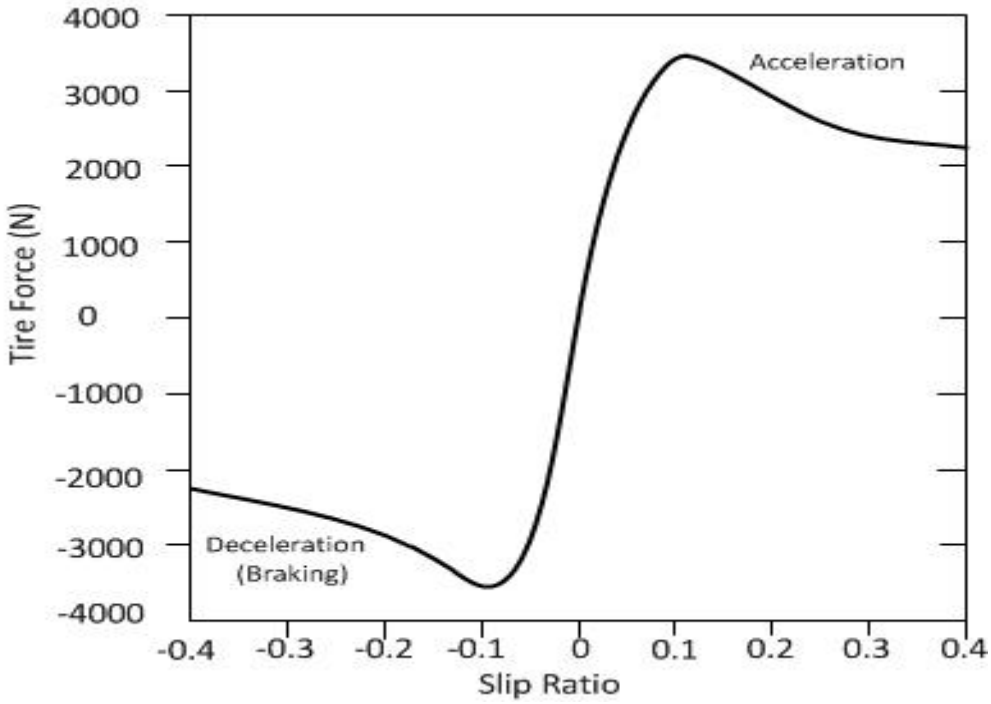

Figure 16: Longitudinal tire force as a function of slip ratio

2.11.3 Rolling resistance

Due to the rotation of the tire, both the tire & the road will suffer some deformation in their contact patch. Because the road has the characteristics of being stiffer, its deformation can easily be neglected. On the contrary, the material of the tire is much more elastic & new material from the tire continuously enters the contact patch as the tire rotates. Normal load causes the vertical deflection of the material while rotating over the contact patch. Then, after leaving the contact patch, it springs back to its original shape. The material of the tire has the characteristics of internal damping. Consequently, the energy that is consumed in the deformation of the tire material is not completely recovered when the material comes back to its original shape. This energy loss can be explained by the term ‘’ rolling resistance’’ which is practically a force that acts on the tires. Consequently this force opposes the motion of the vehicle. The rolling resistance & the normal force which acts on the tire are in proportional to each other as shown in the equation (2.40)

The rolling resistance is proportional to the normal force acting on tire.

$$R_{fr} = f.F_{zr} \tag{2.40}$$

Where f is the rolling resistance Coefficient. And it varies in the range of 0.01 to 0.04.

2.11.4 Calculation of normal tire forces

It is supposed that the weight of the vehicle is distributed equally over each wheel and the calculation of tire load can be done by considering the $\sum T = 0$ about the point which is the contact point of tire and ground to derive the normal tire force on the front left wheel, the $\sum T = 0$ should be written about rear contact point.

.

$$F_{zfl}(l_r + l_f) + \left(\frac{M}{2}\right) r\ddot{\theta_m} h + \left(\frac{M}{2}\right) g.sin\alpha.h - \left(\frac{m}{4}\right) g.cos\alpha.(l_r + l_f) = 0 \quad (2.41)$$

Where:

h is the height of vehicle's central mass, m

$\ddot{\theta_m}$ is the rotational acceleration of the HM, rad/s^2

$$F_{zfl} = \frac{-\left(\frac{M}{2}\right).(r\ddot{\theta_m})h - \left(\frac{M}{2}\right)g.sin\alpha.h + \left(\frac{m}{4}\right)g.cos\alpha.(l_r+l_f)}{l_r+l_f} \quad (2.42)$$

To derive the normal tire force on the rear wheel, the equation of $\sum T = 0$ should be written about front contact point.

$$F_{zrl} = \frac{\left(\frac{M}{2}\right).(r\ddot{\theta_m})h + \left(\frac{M}{2}\right)g.sin\alpha.h + \left(\frac{m}{4}\right)g.cos\alpha.(l_r+l_f)}{l_r+l_f} \quad (2.43)$$

Then the rolling resistance force can be written as

$$R_{fr} = f.\frac{-\left(\frac{M}{2}\right).(r\ddot{\theta_m})h - \left(\frac{M}{2}\right)g.sin\alpha.h + \left(\frac{m}{4}\right)g.cos\alpha.(l_r+l_f)}{l_r+l_f} \quad (2.44)$$

The value of the rolling resistance coefficient f varies in the range 0.01 to 0.04.

2.11.5 Wheel Dynamic

For the driving wheels (for example, right wheel from the front axle), the dynamic equation for the wheel rotational dynamics is:

$$J_{tr}.\ddot{\theta_{fr}} = T_w - r.F_{fr} \tag{2.45}$$

F_{fr} is the longitudinal tire force and can be defined by:

$$\left(\frac{M}{2}\right)\ddot{x} = F_{fr} + F_{rr} - R_{fr} - R_{rr} - \left(\frac{M}{2}\right)gsin(\alpha) \tag{2.46}$$

$$2\ F_{fr} = \left(\frac{M}{2}\right)\ddot{x} + (R_{fr} + R_{rr}) + \left(\frac{M}{2}\right)gsin(\alpha) \tag{2.47}$$

Where

$F_{fr}\ is$ the longitudinal force of front − right tire, N

$F_{rr}\ is$ the longitudinal force of rear − right tire, N

$R_{fr}\ is\ the\ rolling\ resistance\ force\ of\ front - right\ tire, N$

$R_{rr}\ is\ the\ rolling\ resistance\ force\ of\ rear - right\ tire, N$

If (2.44) be substituted in (2.47) then:

$$F_{fr} = \left(\frac{M}{4}\right)r.\ddot{\theta_{fr}} + f.(\left(\frac{m}{4}\right)g.cos\alpha) + \left(\frac{M}{4}\right)gsin(\alpha) \tag{2.48}$$

Then T_w which is the torque created by HM is equal with

$$T_w = \eta_{\mathrm{hmm}}.\varepsilon_m.V_m.\Delta p \tag{2.49}$$

The hydro mechanical efficiency coefficient (η_{hmm}) like other efficiencies coefficient is depended on pressure and also rotational velocity of HM.

If we substitute (2.49) and (2.48) in (2.45) then

$$J_{tr}.\ddot{\theta_{fr}} = \eta_{\text{hmm}}.\varepsilon_m.V_m.\Delta p - r.\left[\left(\frac{M}{4}\right)r.\ddot{\theta_{fr}} + f.\left(\left(\frac{m}{4}\right)g.cos\alpha\right) + \left(\frac{M}{4}\right)gsin(\alpha)\right] \quad (2.50)$$

If we write the equation in another form then the angular acceleration of the front right wheel can be calculated.

$$\ddot{\theta_{fr}}\left(J_{tr} + r^2\left(\frac{M}{4}\right)\right) = \eta_{\text{hmm}}.\varepsilon_m.V_m.\Delta p - f.r.g\left(\frac{M}{4}\right)cos\alpha - r.g\left(\frac{M}{4}\right)sin\alpha \quad (2.51)$$

And finally the angular acceleration of the front right wheel is:

$$\ddot{\theta_{fr}} = \frac{\eta_{\text{hmm}}.\varepsilon_m.V_m.\Delta p}{\left(J_{tr}+r^2\left(\frac{M}{4}\right)\right)} - \frac{f.r.g\left(\frac{M}{4}\right)cos\alpha}{\left(J_{tr}+r^2\left(\frac{M}{4}\right)\right)} - \frac{r.g\left(\frac{M}{4}\right)sin\alpha}{\left(J_{tr}+r^2\left(\frac{M}{4}\right)\right)} \quad (2.52)$$

The angular acceleration of the front left wheel is:

$$\ddot{\theta}_{fl} = \frac{\eta_{\text{hmm}}.\varepsilon_m.V_m.\Delta p}{\left(J_{tl}+r^2\left(\frac{M}{4}\right)\right)} - \frac{f.r.g\left(\frac{M}{4}\right)cos\alpha}{\left(J_{tl}+r^2\left(\frac{M}{4}\right)\right)} - \frac{r.g\left(\frac{M}{4}\right)sin\alpha}{\left(J_{tl}+r^2\left(\frac{M}{4}\right)\right)} \quad (2.53)$$

These equations can be used to build the Simulink model in MATLAB.

2.12 model validation

In this section the validation of the calculated simple dynamic model is tested and is compared with IHA machine's response. As we explained earlier whenever we talk about the IHA machine, the data obtained by simulator (Gimsim) is meant. The dynamic model is based on simple model, section (2.9). The comparisons are made on gradient & smooth (horizontal) terrains.

2.12.1 Optimization Unit

As it is shown in the figure 17 the task of optimization block is to set the manipulated variables which are diesel engine rpm and pump displacement setting for a specific desired velocity. The optimization block plays the role of an open loop controller in the system.

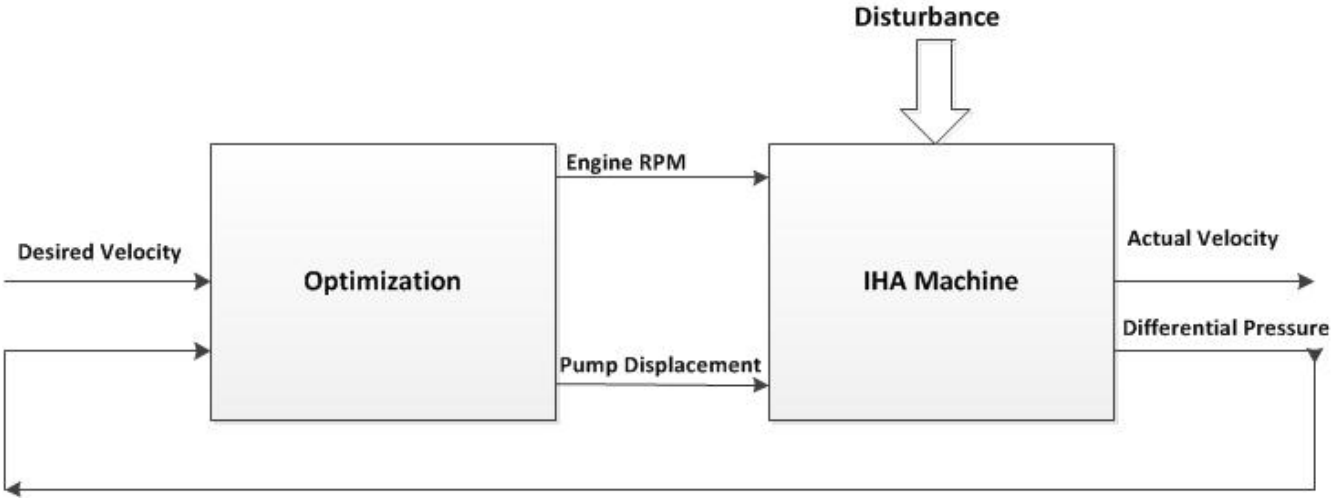

Figure 17: Optimization block

We consider a specific desired velocity as an input to the optimization block to check the performance of the block which sets the manipulated variables. As shown in the figure 18 the desired velocity is about 9 km/h and the pump displacement setting is set about 0.8 and diesel engine rpm is constant at 1000 rpm. According to the optimization unit's strategy, to reduce the fuel consumption for a specific desired velocity the pump displacement setting must be as high as possible and the diesel engine rpm must be as low as possible. The reason behind this logic is due to the higher fuel consumption of diesel engine rpm in comparison with pump displacement setting modification.

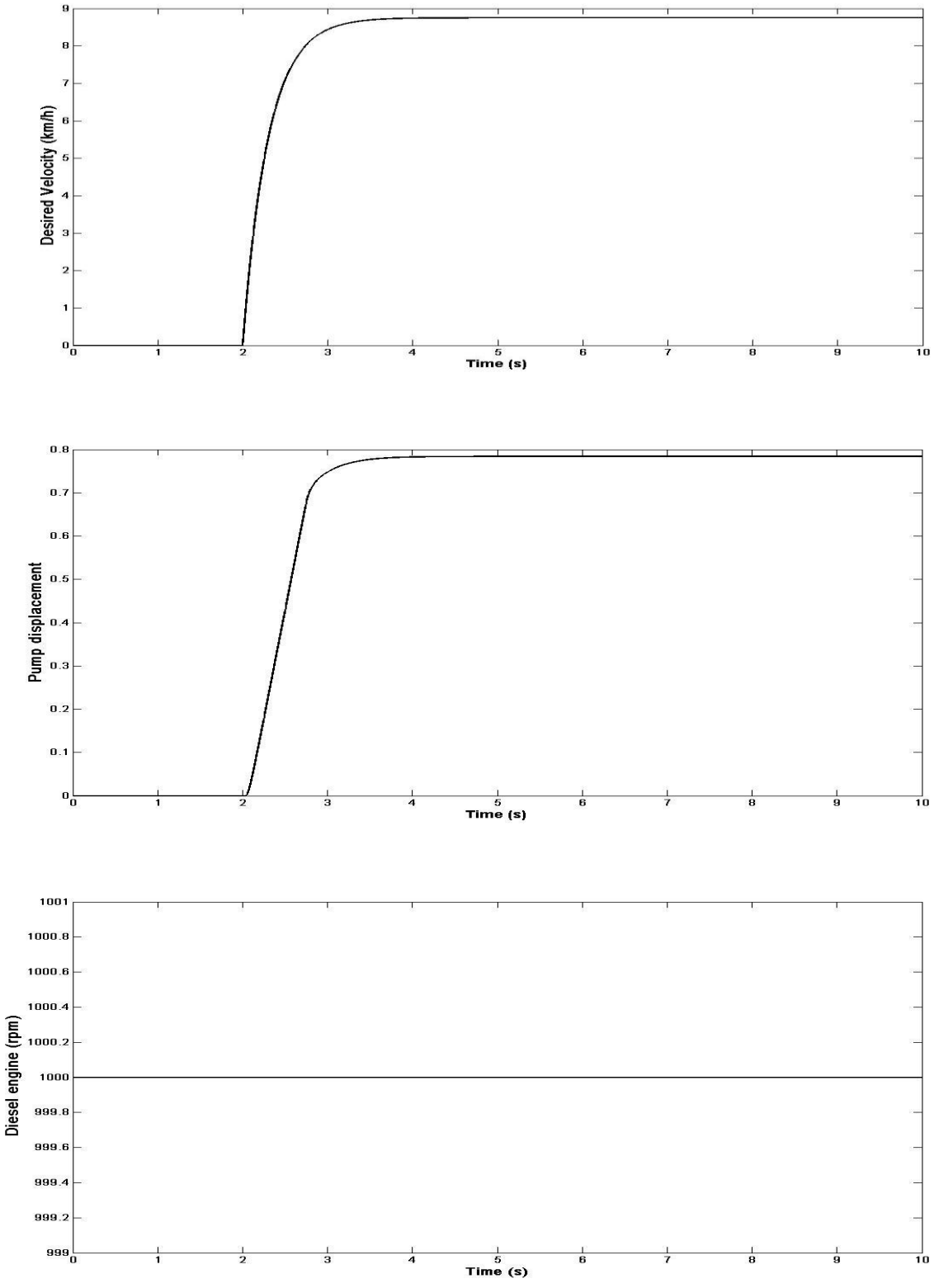

Figure 18: Pump displacement & engine rpm set by optimization block

2.12.2 Open loop controller

The figure 19 shows the velocity comparison between IHA machine (Gimsim) & its Dynamic model in an open loop structure. The terrain is considered to be smooth and horizontal. The green curve demonstrates the Simulator (Gimsim) data & the red curve shows the calculated dynamic model data (section 2.9).

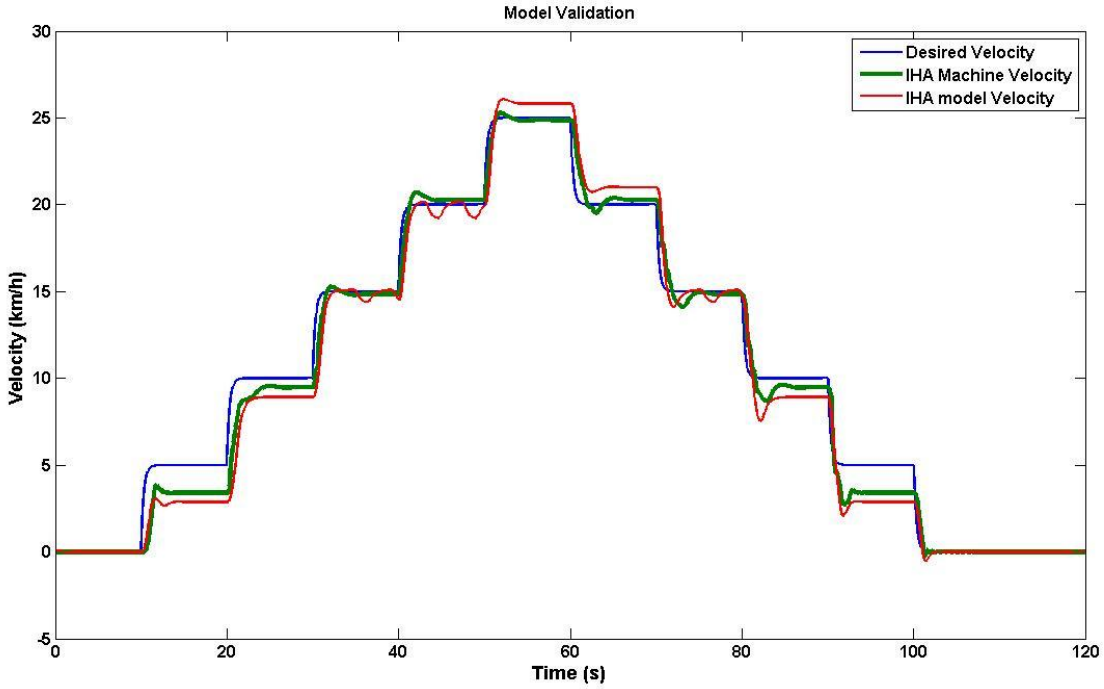

Figure 19: IHA machine & its dynamic model velocity comparison on smooth terrain

The figure 19 shows that the validity of the dynamic model can be confirmed because it follows the IHA machine's response quite closely. There is a tracking error about 1 (km/h) between model's response and Machine's response at low speed and when the desired velocity increases the tracking error decreases. The tracking error is due to the problem in the optimization block. The possible solution to avoid **oscillation and tracking error** in the optimization unit is discussed in the Appendix C. The dynamic model is based on simple model, section (2.9).

In the figure 20 the dynamic model is tested on a gradient terrain with 10 degree slop and the result is compared with the IHA machine's (Gimsim) response. With considering that both of them have open loop control system.

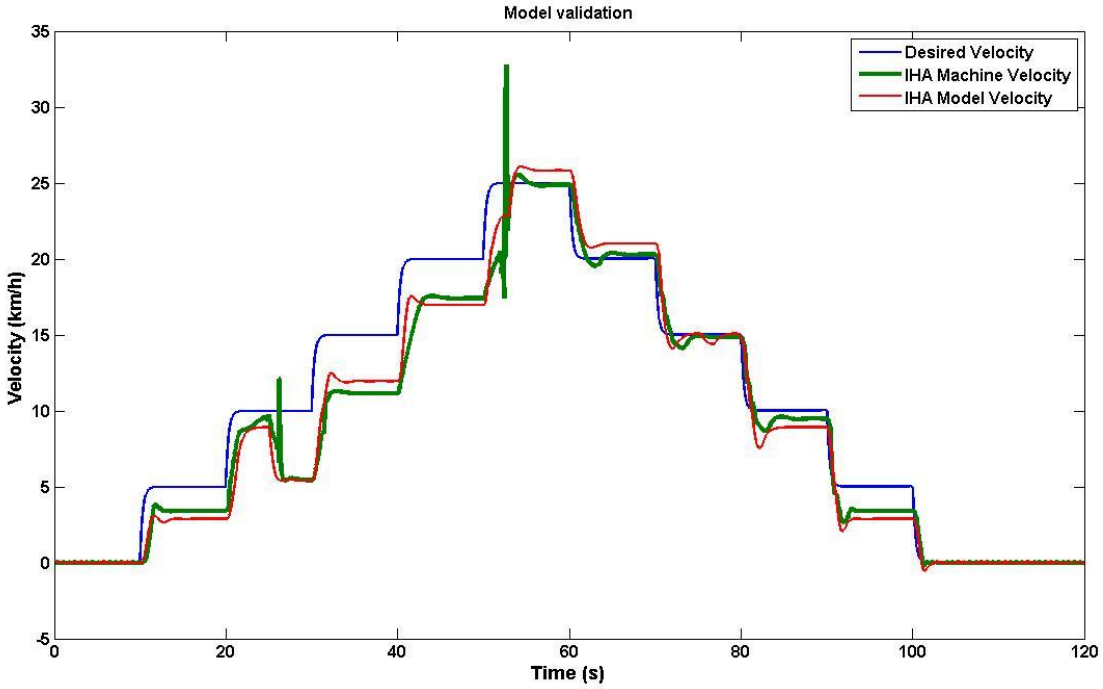

Figure 20: IHA machine & its dynamic model velocity comparison on gradient terrain

The machine enters the gradient terrain between the time (25-53) s. as the figure 20 shows the dynamic model's response follows the IHA machine's response on a gradient terrain satisfactorily.

As the green curve shows, the spikes happen in entrance and exit of the ramp. The error of measurement in velocity sensor which is connected to the wheel is the reason of spikes in data. The red curve does not show the spikes because the Tire-terrain interaction & sensors are not modeled in the dynamic model.

3.0 Control

Different methods of controlling like Model base predictive control and gain-scheduled PID control were tested for cruise control of the IHA machine. Dynamic characteristic of the hydraulic systems are nonlinear and a single controller cannot cover the entire range of operation. Huhtala, K [12] showed that gain-scheduled PI control can provide a sufficient control over the entire operating range of Unit. He has designed an upper level controller which determines the command values for the controllers of the diesel engine, hydrostatic pump and motor depending on the operating point of the HST.in his design he has used fixed PI-controllers which are tuned at two different operating ranges. The operating ranges are the low speed and high speed of the units. According to Huhtala, K [12]'' one significant problem in designing the control of a diesel engine, hydrostatic pump and motor is the changing dynamic characteristic of velocity control. The natural frequency, damping ratio and gain change are functions of the displacement setting of the pump and motor and rotational speed of the pump. It is because of this that a controller with fixed gain cannot achieve optimal control over the entire range of operation.'' The gain scheduling is based on the rotational velocity of motor. Although the same fixed PID-control is used in our design, the gains are tuned in different operating ranges. Three different gains are defined for three different operating ranges of the motor at low, intermediate & high speed.

3.1 Control Structure

As the figure 21 shows, a feedback control is added to the open loop structure to remove the error caused by Disturbance.

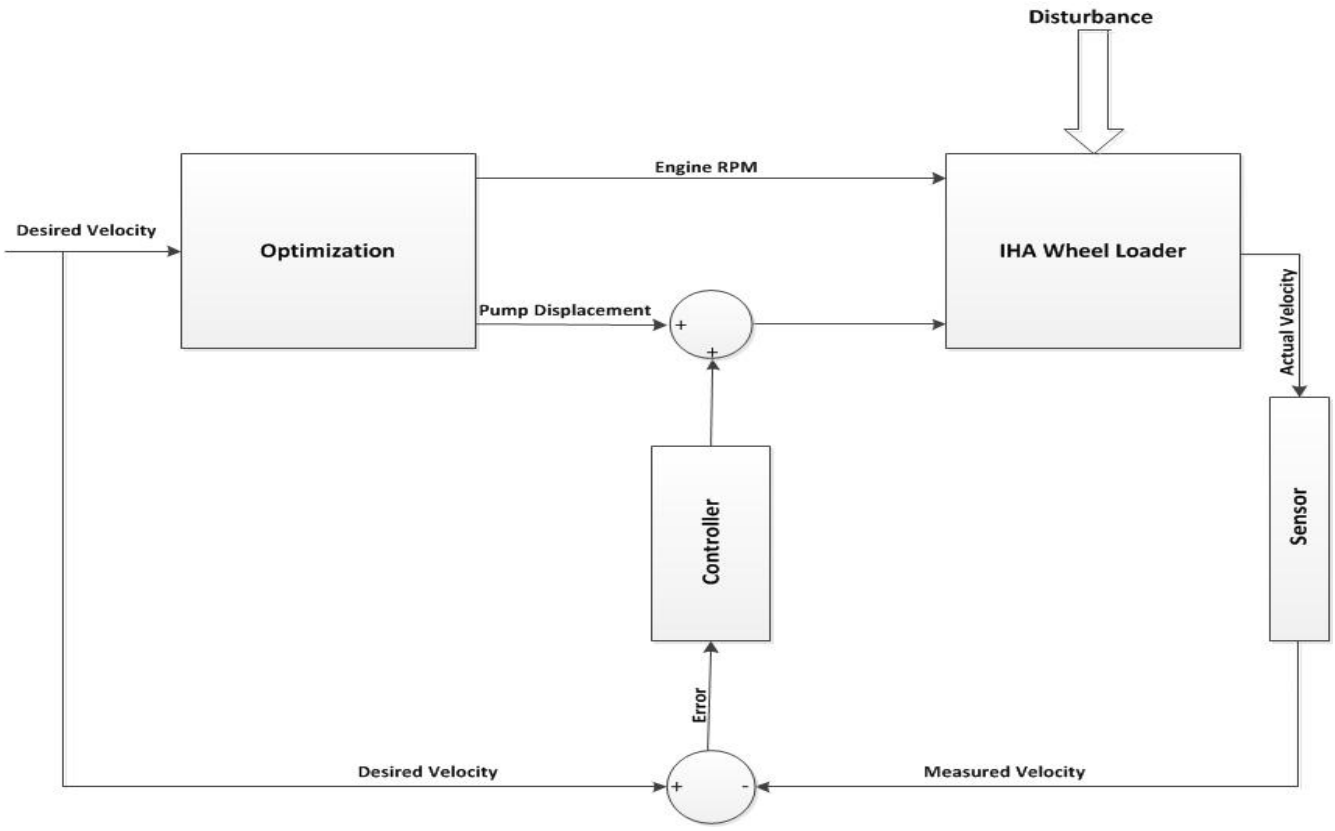

Figure 21: control Structure

The pump displacement setting is the only manipulated variable which the controller can modify it as an input to the plant to remove the error between the desired velocity and measured velocity. The diesel engine rpm is set by optimization block and the controller cannot modify it. The disturbance can cause error between the desired and measured velocity. The gradient terrain is external disturbance. It will be discussed later in the section (3.4) how the feed forward controller can remove the transient error in the feedback control system.

The type of the controller is gain-scheduled discrete PID-Controller which the gains are changed by gain scheduling. The gain scheduling is based on the rotational velocity of the motor which is a state space variable of the dynamic model. Three PID-controllers with different gain have been defined for slow, intermediate and high speed of the motor. The gain of the PID- controller needs to be retuned because the dynamic characteristic of the model changes in different speed range. The gain-scheduled controller is designed so that its operation is equivalent to near optimal operation of a PID-controller with fixed parameters in different speed ranges and different tunings.

3.2 Dynamic model linearization

We need to linearize the nonlinear dynamic model over different operating points to be able to design the closed loop controllers. The input of the system is considered to be Pump Displacement ($\in_p$) and the output of the system is actual velocity of the machine (V_x). The cruise control is only dependent on the pump's volumetric displacement setting. The required Diesel engine rpm is set by optimization unit according to the required power.

The figure 22 shows the open loop structure of the system between pump displacement setting as an input and actual velocity as an output. The transfer function of the plant can be obtained by linearizing the model between the points of 1 & 2.

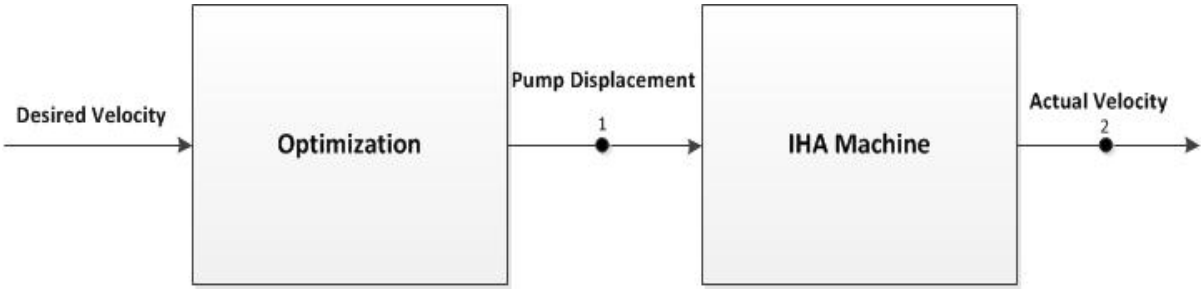

Figure 22: Open loop controller's structure

The motor rotational velocity and pressure are two state space variables which are used to linearize the model. The operating points of state space variables are defined for linearization in three different values.

The values of motor rotational velocity variable are (0-25), (25- 50) & (50-100) rpm which are considered as low, intermediate and high velocity. The value of pressure as another state space variable is considered to be about (0-350) bars for all three different velocities. Three different open loop transfer function is calculated for three different velocity (low, Intermediate and high).To verify the stability of the system, the bode stability criterion is examined. the bode stability criterion is examined for three calculated open loop transfer functions which are in series with the PID controller's transfer functions estimated in the section (3.3).

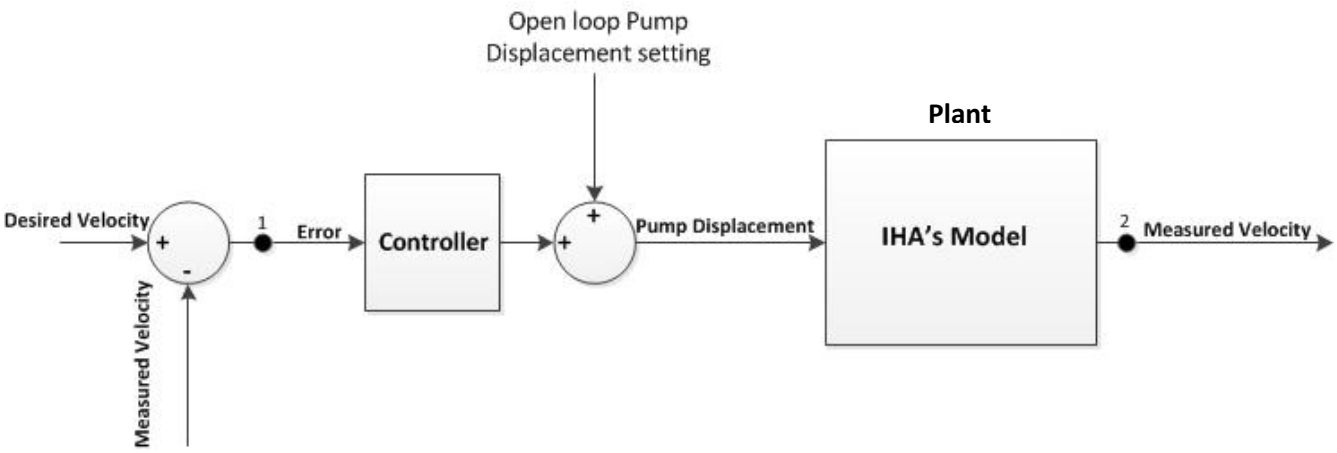

Figure 23: open loop circuit for testing Bode instability criterion

According to the Bode instability criterion:

. The phase crossover frequency, ω_{pc}, is the frequency where phase shift is equal to -180^{o}.

. The gain crossover frequency, ω_{gc}, is the frequency where the amplitude ratio is 1, or when log modulus is equal to 0.

If at the phase crossover frequency, the corresponding log modulus of M(iω_{pc}) is less than 0 dB, then the feedback system is stable.

When a nonlinear dynamic model is linearized several linear models can be calculated for the specific operating points. Each linear model has its own transfer function which can be considered as the representative of other transfer functions in the specific operating range. Three regions as three operating ranges (low, intermediate and high motor velocity) are shown in the figure 24 only one transfer function is selected for each region. The controller should be able to cover the entire range of operation for each region. The bode instability criterion test can be used to check the instability of the system for each region with specific controller.

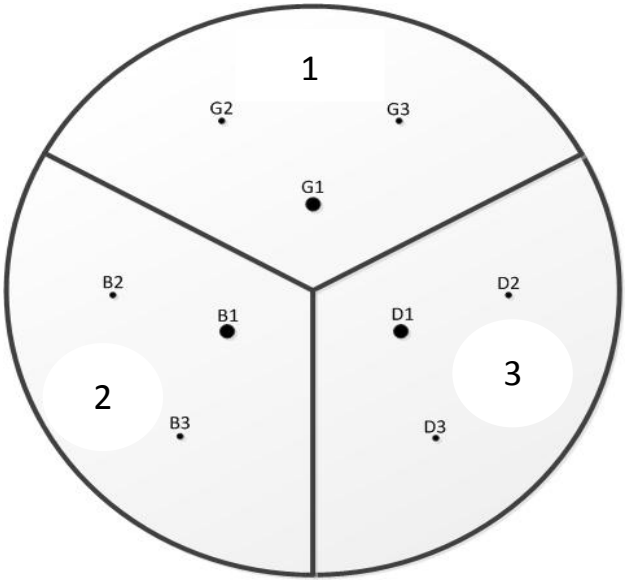

Figure 24: Three operating range

As we explained before only one transfer function as a representative of other transfer functions in each region is selected. The system exists at equilibrium point for the first region when

$\frac{d\Delta p}{dt} = \ddot{\theta_m} = 0\,,\ \Delta p = \dot{\theta}_m \cong 0$

The first transfer function of plant after linearization for low velocity is:

$$G1 = \frac{28.75}{s^2 + 4.346\,s + 10.38} \tag{3.1}$$

The unit of the transfer function is $\frac{km}{h}$

The first transfer function of plant and controller C1 in series is:

$$G = \frac{100.2\,s^2 + 244\,s + 878}{s^4 + 29.35\,s^3 + 119\,s^2 + 259.5s} \tag{3.2}$$

The unit of the transfer function is $\frac{km}{h}$

As the Figure 25 shows according to the Bode criterion stability all the transfer functions of linearized models in the region 1 which are in series with controller C1 are stable.

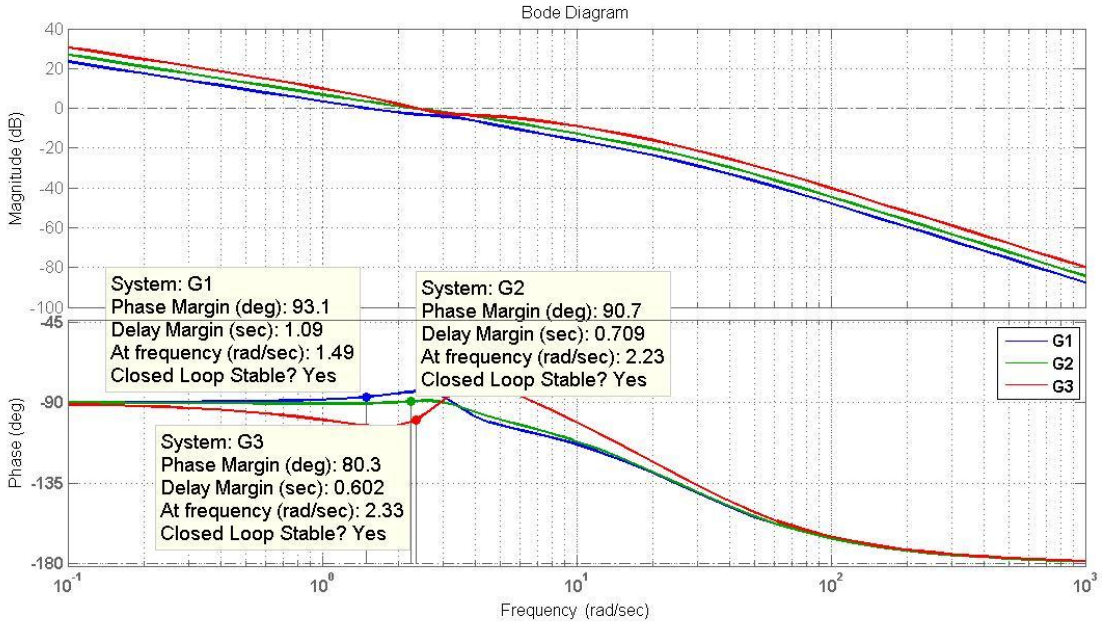

Figure 25: bode diagram for the first region

The system exists at equilibrium point for the second region when

$\frac{d\Delta p}{dt} = \ddot{\theta_m} = 0\,,\ \Delta p \cong 0\,, \dot{\theta}_m \cong 25\ rpm$

The second transfer function of plant after linearization for intermediate velocity is:

$$B1 = \frac{120.9}{s^2 + 7.772\ s + 11.03} \tag{3.3}$$

The unit of the transfer function is $\frac{km}{h}$

The second transfer function of plant and controller C2 in series is:

$$B = \frac{697.5\ s^2 + 2536\ s + 1.126\times10^4}{s^4 + 32.77\ s^3 + 205.3\ s^2 + 275.8s} \tag{3.4}$$

The unit of the transfer function is $\frac{km}{h}$

As the Figure 26 shows according to the Bode criterion stability all the transfer functions of linearized models in the region 2 which are in series with controller C2 are stable.

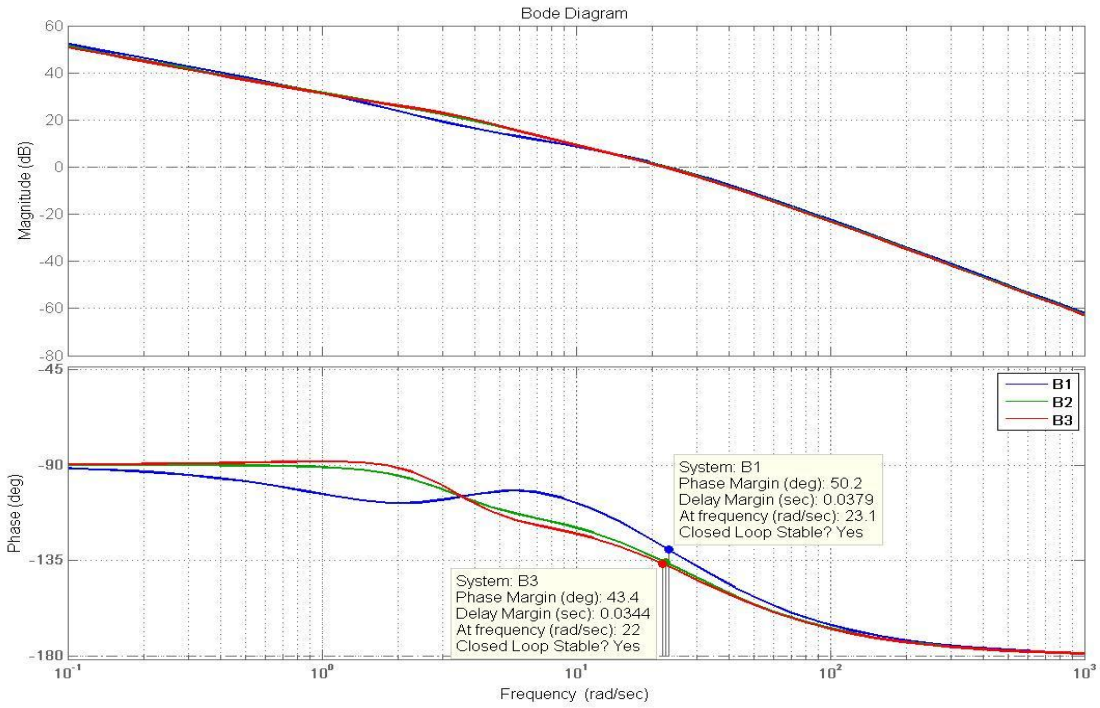

Figure 26: bode diagram for the second transfer function

The system exists at equilibrium point for the third region when

$\frac{d\Delta p}{dt} = \ddot{\theta_m} = 0\,,\ \Delta p \cong 0\,, \dot{\theta}_m \cong 50\,rpm$

The third transfer function of plant for high velocity after linearization is:

$$D1 = \frac{219.1}{s^2 + 7.65\,s + 11.37} \tag{3.5}$$

The unit of the transfer function is $\frac{km}{h}$

The third transfer function of plant and controller C3 in series is:

$$D = \frac{1527\,s^2 + 5101\,s + 2.126 * 10^4}{s^4 + 32.65\,s^3 + 202.6\,s^2 + 284.3s} \tag{3.6}$$

The unit of the transfer function is $\frac{km}{h}$

As the Figure 27 shows according to the Bode criterion stability all the transfer functions of linearized models in the region 3 which are in series with controller C3 are stable.

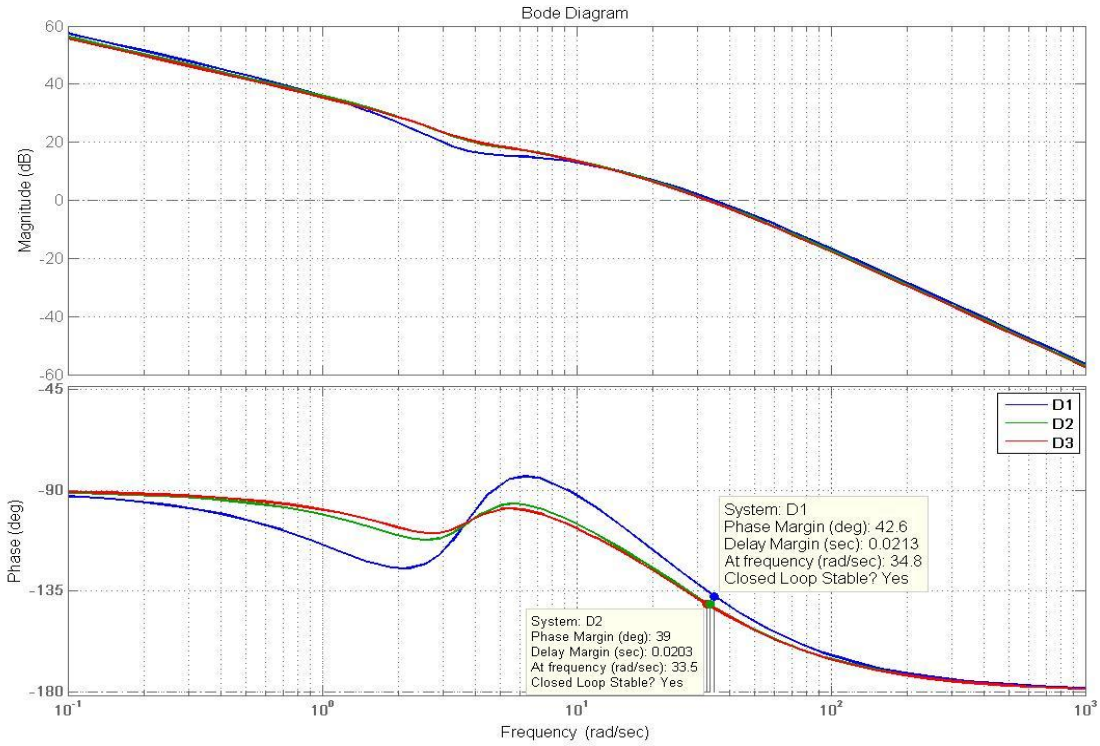

Figure 27: bode diagram for the third transfer function

3.3 Closed loop controller's structure

The figure 28 shows the closed loop controller's structure:

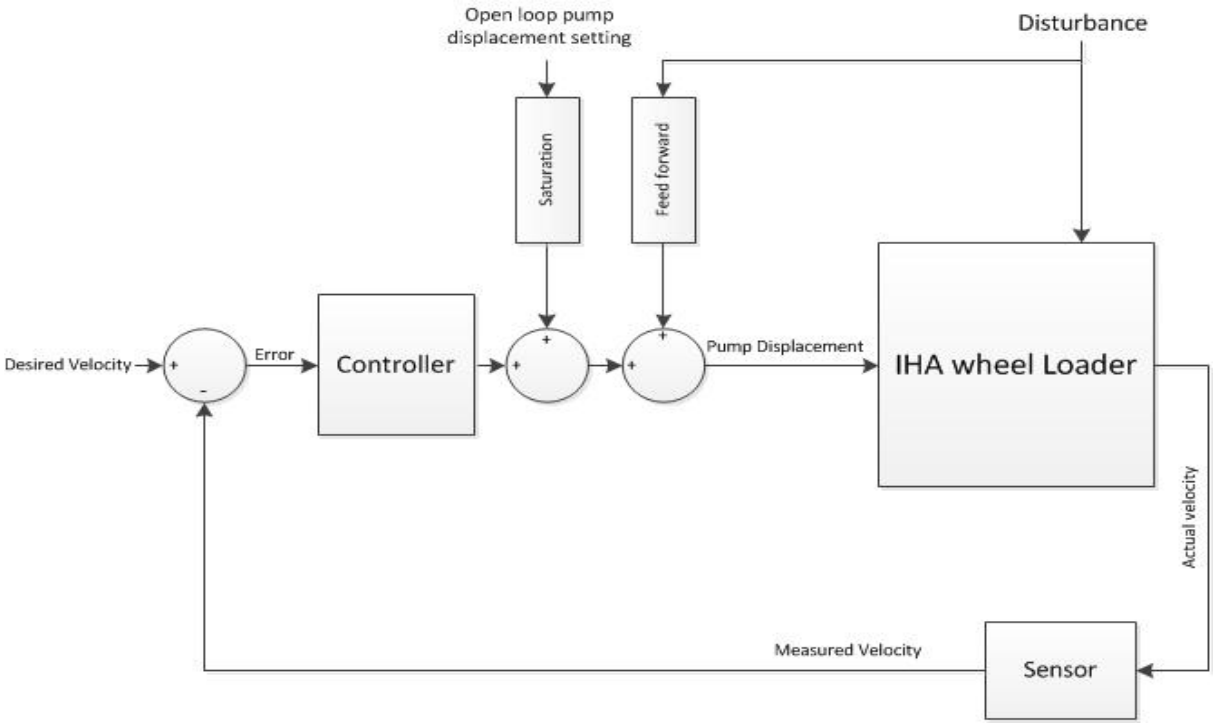

Figure 28: closed loop controller's structure

The input of the closed loop control system is desired velocity and the output is the measured velocity. The external disturbance is tried to be rejected by using feed forward gain.

The open loop pump displacement setting is saturated to $\pm$ 0.8 of its total value and the controller is considered to provide $\pm$ 0.2 of the rest. The reason of saturation is the speed tracking error problem in the optimization unit. Transfer function of the sensor is considered to be 1. The Ziegler-Nichols tuning method is used for a primary guess to set the controller's gain.

The general form of PID-controller's transfer function is:

$$\mathbf{P=}\ \frac{\mathbf{k_P.\left(T_i.T_d.s^2+T_i.s+1\right)}}{\mathbf{T_i s}}$$

The controller transfer function does not have unit because it converts the error to pump displacement setting which both don't have unit.

The PID-controller gains are listed in the Table 4:

Table 4: PID-Controller gains

PID gains / Controller number	Kp	Ti	Td	Filter coefficient
1th controller	0.7267	3.0538	0.3196	0.04
2th controller	0.86267	4.65538	0.25396	0.04
3th controller	0.97	4.8505538	0.3096	0.04

The feedback control switches between the three PID-Controller based on the output velocity of HM.

The closed loop transfer function can be obtained while the plant & PID-controller's transfer functions are calculated.

The input of the closed loop control system is desired velocity and the output is measured velocity.

The first closed loop transfer function for low velocity is:

$$\mathbf{T1} = \frac{100.2s^2+244s+878}{s^4+29.35\,s^3+219.3\,s^2+503.5\,s+878} \quad (3.7)$$

The poles of the model are

P1= -19.1383

P2= -7.9196

P3= -1.1441+2.1175i

P4= -1.1441-2.1175i

& the zero is:

Z1= -1.2173+2.6975i

Z2= -1.2173-2.6975i

The poles and zeros are located at the left side of imaginary axes.

The first step response diagram for low velocity is shown in the Figure 29:

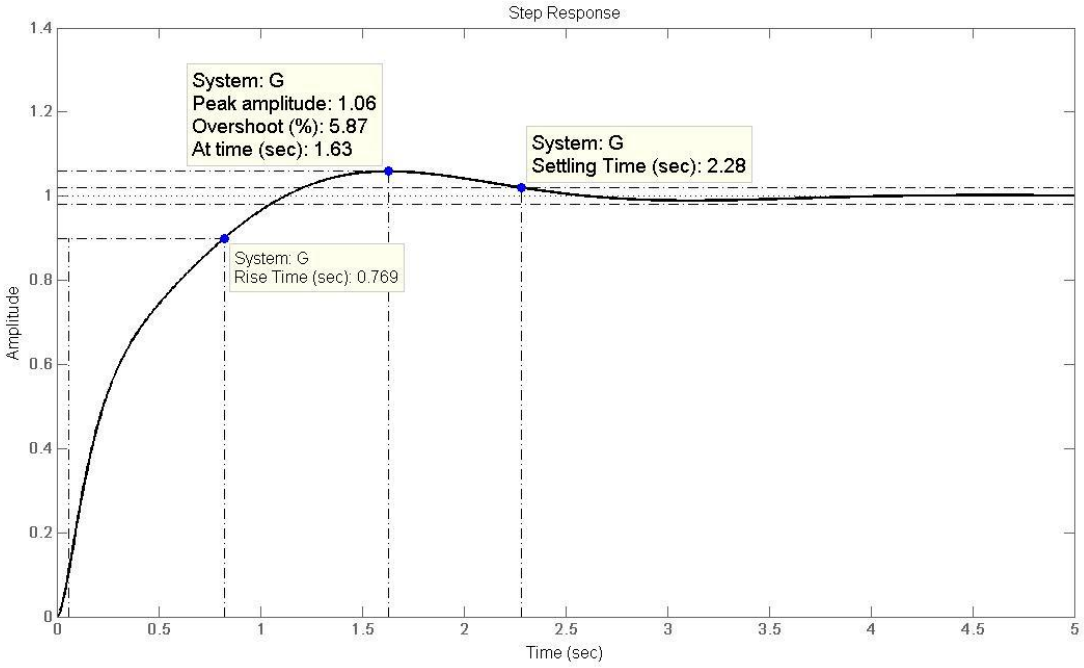

Figure 29: step response diagram of the first closed loop transfer function

As the figure 29 shows the overshoot percent of the first controller's response is 5.87 % and the settling time is 2.28 (s). The criterion of 2% is considered for the settling time. Because the leakage in the hydraulic circuit is much higher at low speed the dynamic behavior of the machine is over damped and it can cause a larger settling time for the step response.

The second closed loop transfer function for intermediate velocity is:

$$\mathbf{T2=}\ \frac{697.5\,s^2+2536\,s+1.126\times10^4}{s^4+32.77\,s^3+902.8\,s^2+2812\,s+1.126\times10^4} \qquad (3.8)$$

The poles of the model are:

P1= -14.8899+24.0406i

P2= -14.8899-24.0406i

P3= -1.4961 + 3.4407i

P4= -1.4961 - 3.4407i

& the zeros are:

Z1= -1.8180 + 3.5823i

Z2= -1.8180 - 3.5823i

The poles and zeros are located at the left side of imaginary axes.

The second step response for intermediate velocity diagram is shown in the Figure 30:

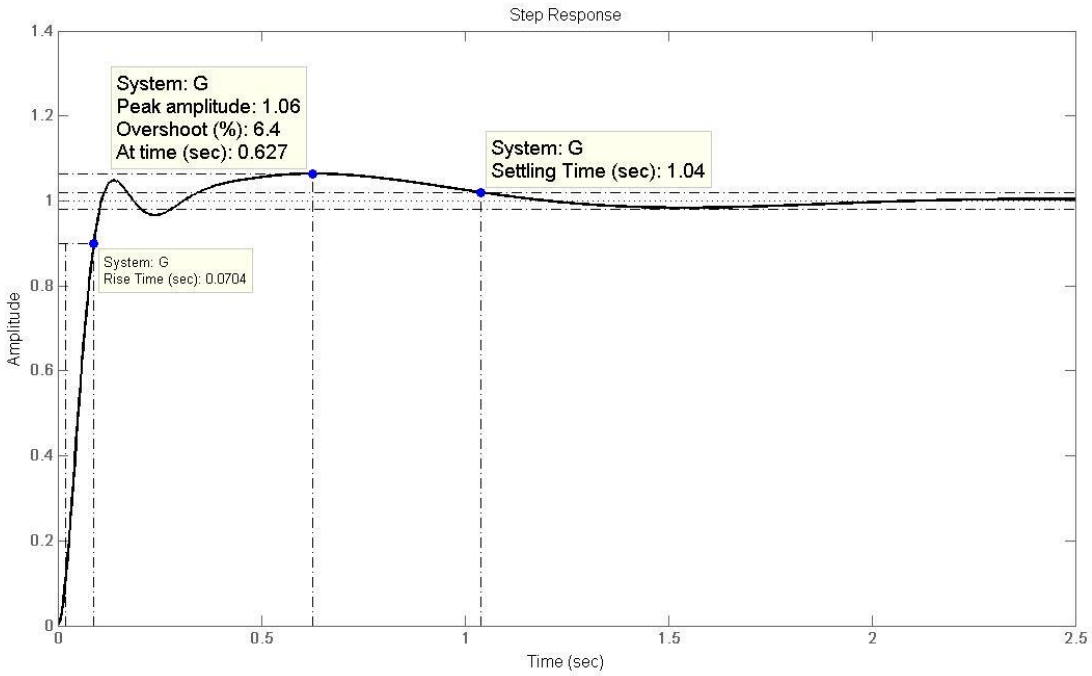

Figure 30: step response diagram of the second closed loop transfer function

As the figure 30 shows the overshoot percent of the second controller's response is 6.4 %. The settling time is 1.04 (s) which is smaller than the first controller's response. The criterion of 2% is considered for the settling time.

The third closed loop transfer function for high velocity is:

$$\mathbf{T3}= \frac{1527\ s^2+5101\ s+2.126\times10^4}{s^4+32.65\ s^3+1729\ s^2+5385\ s+\ 2.126\times10^4} \qquad (3.9)$$

The poles of the model are:

P1= -14.7874 + 37.5049i

P2= -14.7874 - 37.5049i

P3= -1.5376 + 3.2731i

P4= -1.5376 – 3.2731i

& the zero is:

Z1= -1.6705+ 3.3364i

Z2 = -1.6705 – 3.3364i

The poles and zeros are located at the left side of imaginary axes.

The third step response diagram for high velocity is shown in the Figure 31:

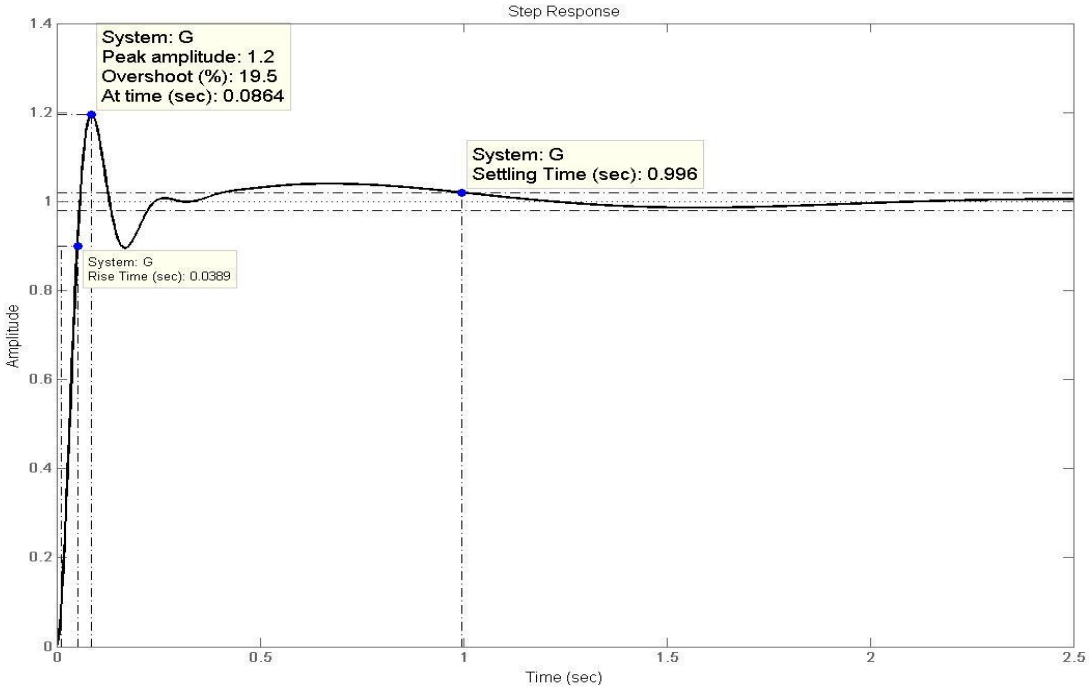

Figure 31: step response diagram of the 3th closed loop transfer function

As the figure 31 shows the overshoot percent for the third controller's response is 19.5 % and settling time is 0.996 (s). Criterion of 2% is considered for the settling time.

3.4 Feed forward

In an ideal case a feed forward control can entirely eliminate the effect of measured disturbance on the system output. Feed forward control can be used along with feedback control to improve the performance of the control system. Feedback control system is required to track the set points changes and to suppress unmeasured disturbances that are always present in any real system and feed forward can remove or minimize the negative effect of measured disturbances on the performance of the system.

The pitch angle of the IHA machine is measured with IMU device. The pitch angle is considered as the measured disturbance and its value becomes nonzero when the machine enters the gradient terrain. The pitch angle is the α angle of the terrain. The relation between slop α and pump displacement setting ε_p is calculated in the equation (3.10).

$$\varepsilon_p = \frac{K_{Tm}.\Delta p}{V_p.\omega_p.\eta_{vp}} + \left(\frac{M.g.r.\dot{\theta_m}}{V_p.\omega_p.\eta_{hmm}.\Delta p.\eta_{vp}}\right).sin\alpha \qquad (3.10)$$

First feed forward equation for low velocity is:

$$\varepsilon_p = 0.0066 + (0.9501 \times sin\alpha)$$

Second feed forward equation for intermediate velocity is:

$$\varepsilon_p = 0.0135 + (1.5470 \times sin\alpha)$$

Third feed forward equation for high velocity is:

$$\varepsilon_p = 0.0138 + (1.7832 \times sin\alpha)$$

The figure 32 demonstrates that a large tracking error happens between the times 23-26 (s). There is only feedback in control system. This happens when the machine enters a ramp with 10 degree Slop.

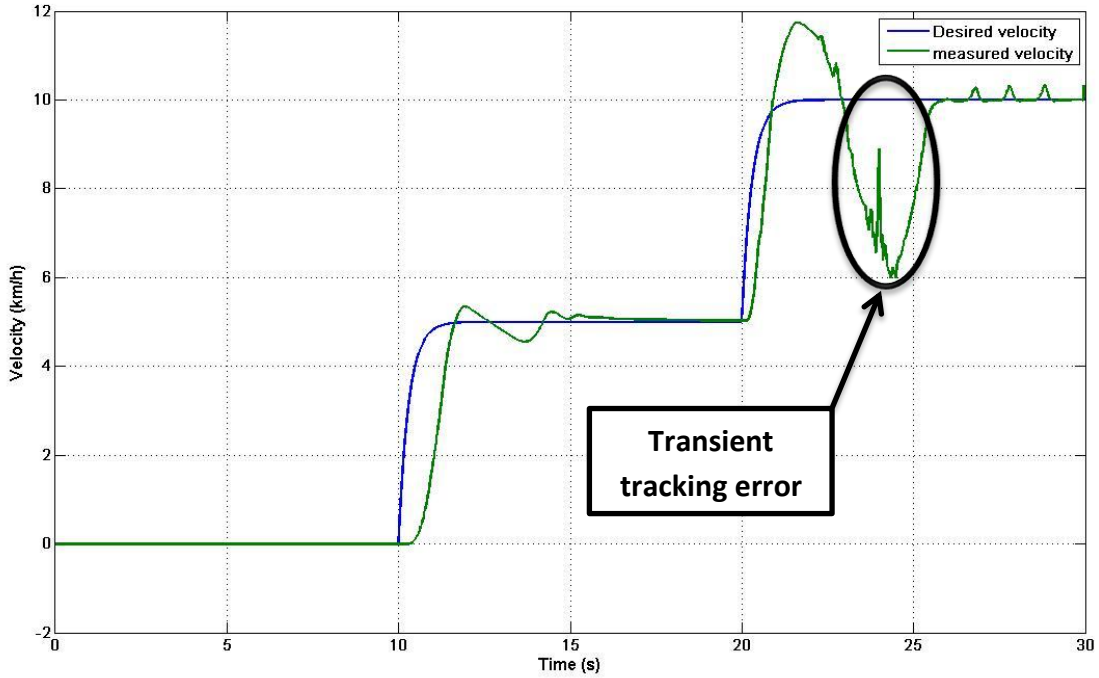

Figure 32: velocity comparison

In practice the feed forward cannot entirely eliminate the effect of external disturbance because of the strategy used in the optimization unit. According to this strategy to reduce the fuel consumption in diesel engine, as the figure 33 shows, the pump displacement should be as high as possible and Diesel engine RPM to be as low as possible. Between the time 23-26 s when the transient tracking error happens, the pump volumetric displacement is almost near to its maximum. In fact the feed forward cannot increase the pump displacement setting anymore and tracking error remains. In practice the feed forward can be useful only in low velocity where the pump displacement is not near 1 because when the pump displacement is saturated to 1 the system becomes open loop. Only the first feed forward gain can reduce the effect of disturbance at low speed when the pump displacement setting is not saturated.

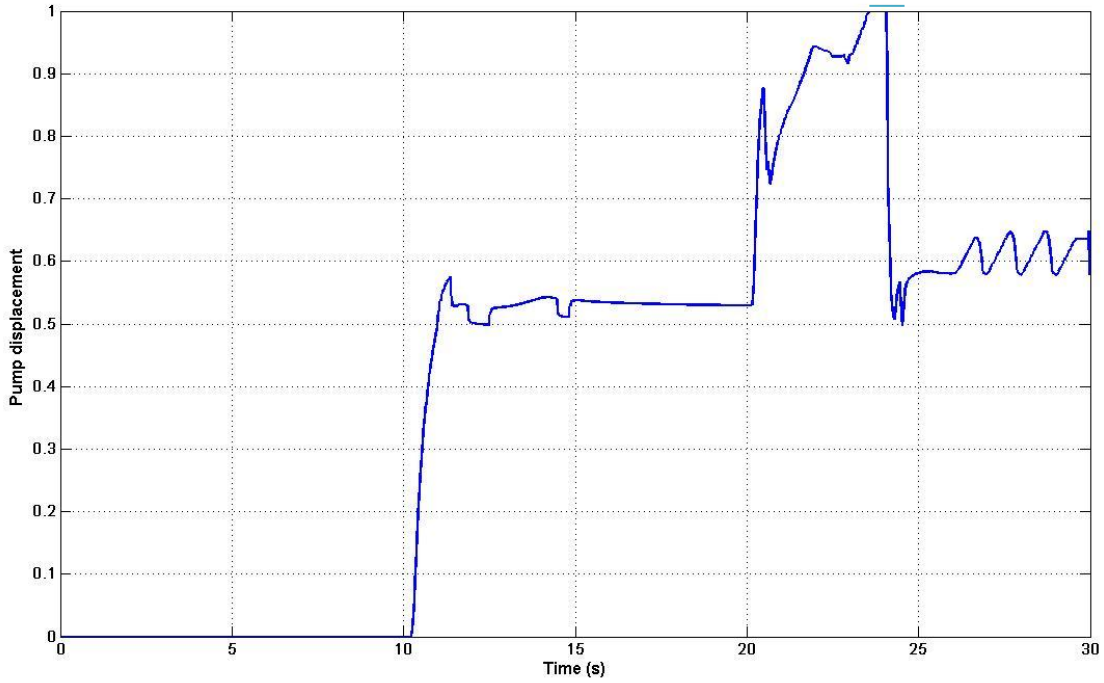

Figure 33: the pump volumetric displacement control in the presence of external disturbance

The diesel engine control is beyond the scope of this thesis and the value is set by the optimization unit. The figure 34 shows the response of diesel engine in the presence of external disturbance.

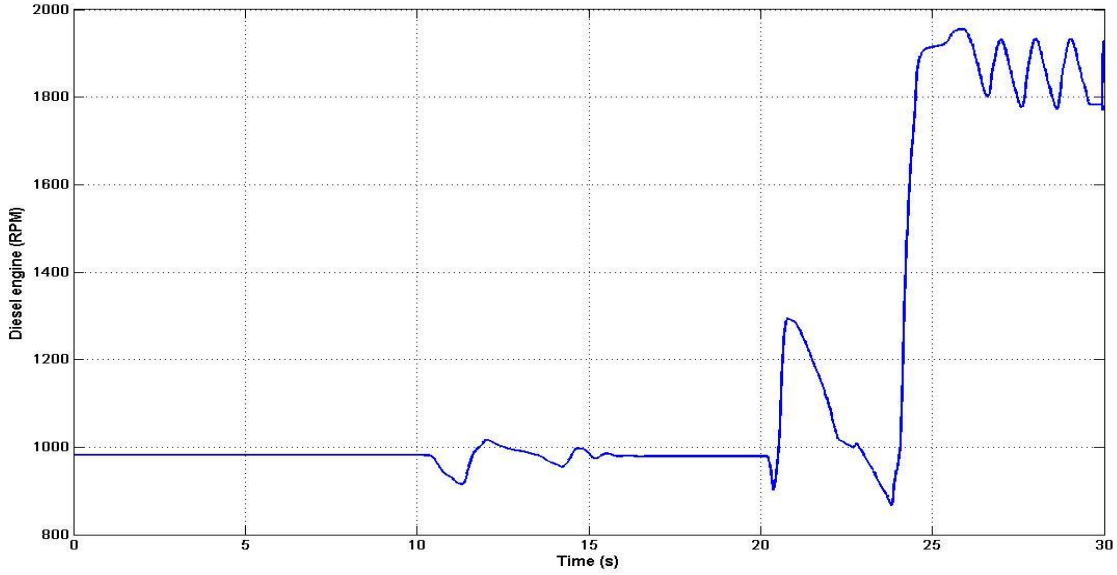

Figure 34: The diesel engine rpm in the presence of external disturbance

As the figure 34 shows the diesel engine is around 1000 rpm at the time 23 s and it takes about 2 second to increase the rpm from 1000 to 2000. In autonomous driving if the physical characteristic of the terrain be unknown, the machine cannot predict the upcoming external disturbance like a ramp. The machine enters the ramp and the IMU device measures the pitch angle which has error and delay and then, the optimization block sets the proper Diesel engine rpm and feedback controller tries to remove the error by modification of pump displacement setting. Both pump and diesel engine have actuating delay and this causes a large tracking error in the cruise control.

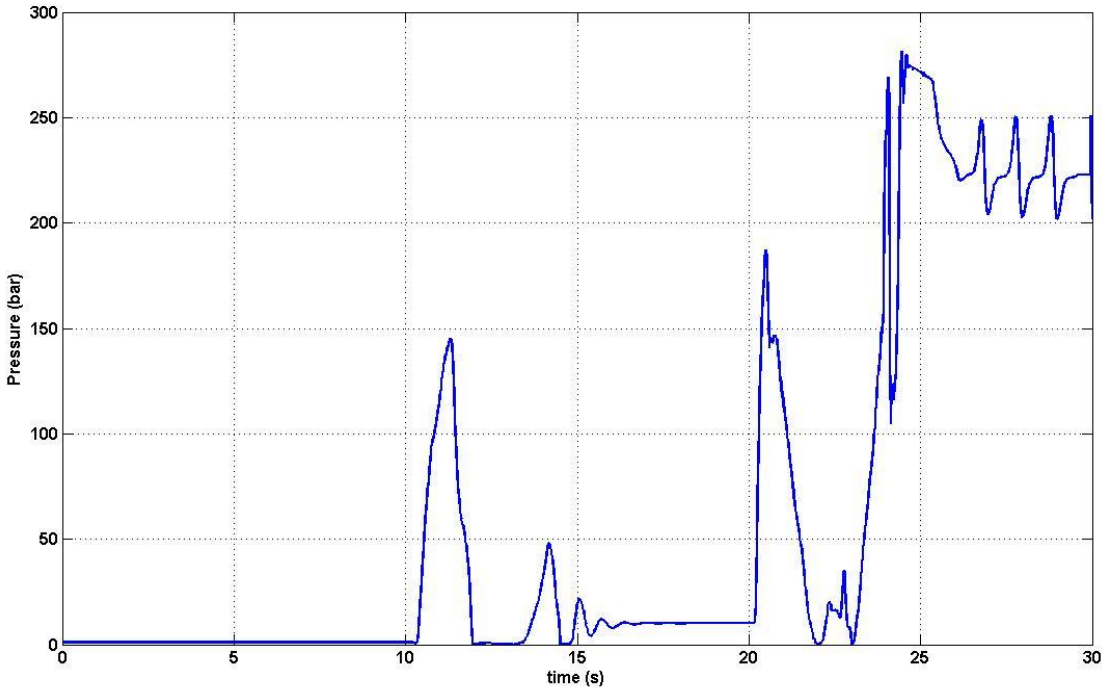

Figure 35: the differential pressure across the main pump

As the figure 35 shows the differential pressure across the main pump increases between the time 23-25 s from 20 to 250 bar. This happens when the machine enters the ramp.

Chapter 4

4.0 wheel loader static test

The real machine is tested in static mode to study the behavior of the hydrostatic power transmission system on a smooth surface and straight line. Pump displacement and diesel engine rpm are two manipulated variables which can control the speed of the machine. In static mode one of manipulated variables is kept constant and the other one is modified and vice versa.

4.1 static test with constant diesel engine rotational speed (rpm)

In the first test the diesel engine rotational speed is kept constant at 1200 rpm and the pump displacement setting is changed from 0 to 100 (%). The figure 36 shows the result:

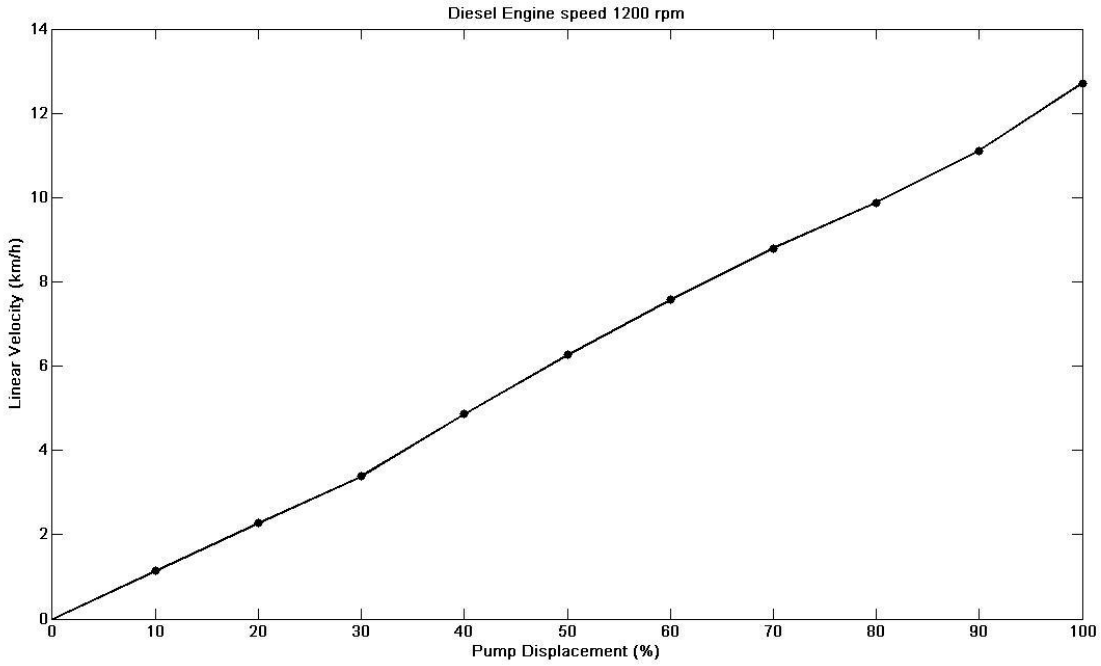

Figure 36: static test with constant diesel engine rotational speed at 1200 rpm

As the figure 36 shows the behavior of the system is almost linear without the presence of external load. The points that are shown in the figure 36 are static points with different pump displacement settings and a constant diesel engine rpm.

Basically the external load has a big influence on the nonlinear behavior of the hydrostatic power transmission and can cause energy loss in the form of leakage flow and friction in the system.

4.1 Static test with fixed pump displacement (60%)

In the second test the pump displacement is kept constant at (60%) and the diesel engine rotational speed is changed from 1100 to 2200 (RPM). The figure 37 shows the result:

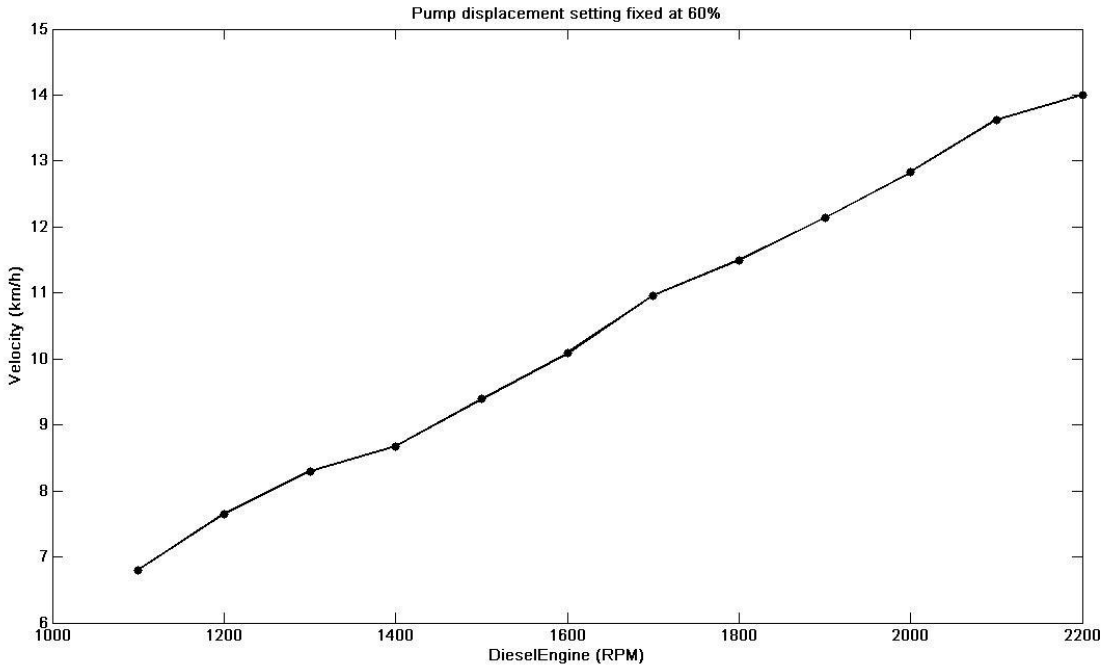

Figure 37: Static test with fixed pump displacement (60%)

This figure 37 shows that the response of the system without the presence of disturbance is almost linear.

The points that are shown in the figure 37 are static points with different diesel engine rotational velocity rpm and a fixed pump displacement setting.

4.2 Articulation radius calculation

Having determined the articulation angle, the articulation radius can be deduced from geometry. Figure 38 shows the geometry of the machine in articulation. It is supposed that the length of the front axle is equal with the length of the rear axle.

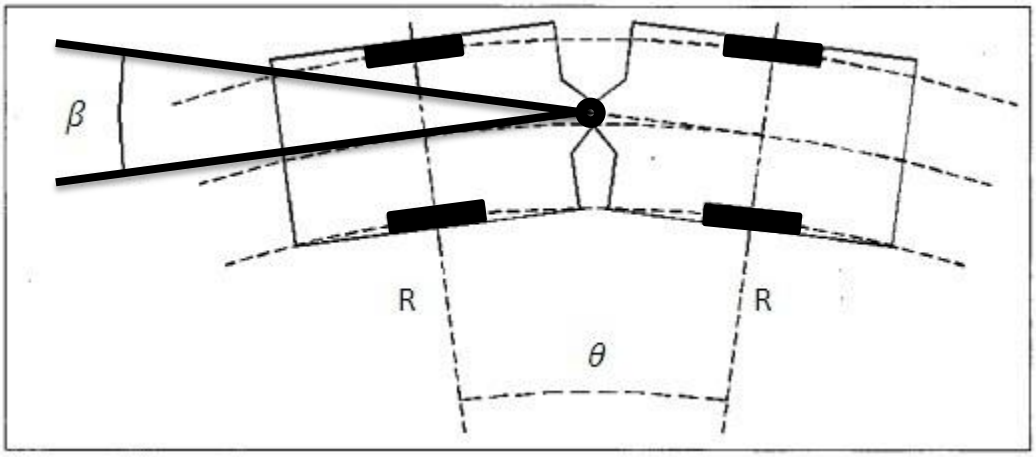

Figure 38: articulation radius calculation

According to the figures 38 & 39:

$$\begin{cases} \beta + \delta = 180 \\ 2\gamma + \theta = 180 \\ 2\alpha + \delta = 180 \\ \alpha + \gamma = 90 \end{cases} \quad (4.1)$$

Then it can be calculated that

$$2\gamma = \delta \quad (4.2)$$

And finally:

$$\beta = \theta \quad (4.3)$$

Now that the articulation angle is determined, the radius of articulation can be calculated as shown in the figure 39.

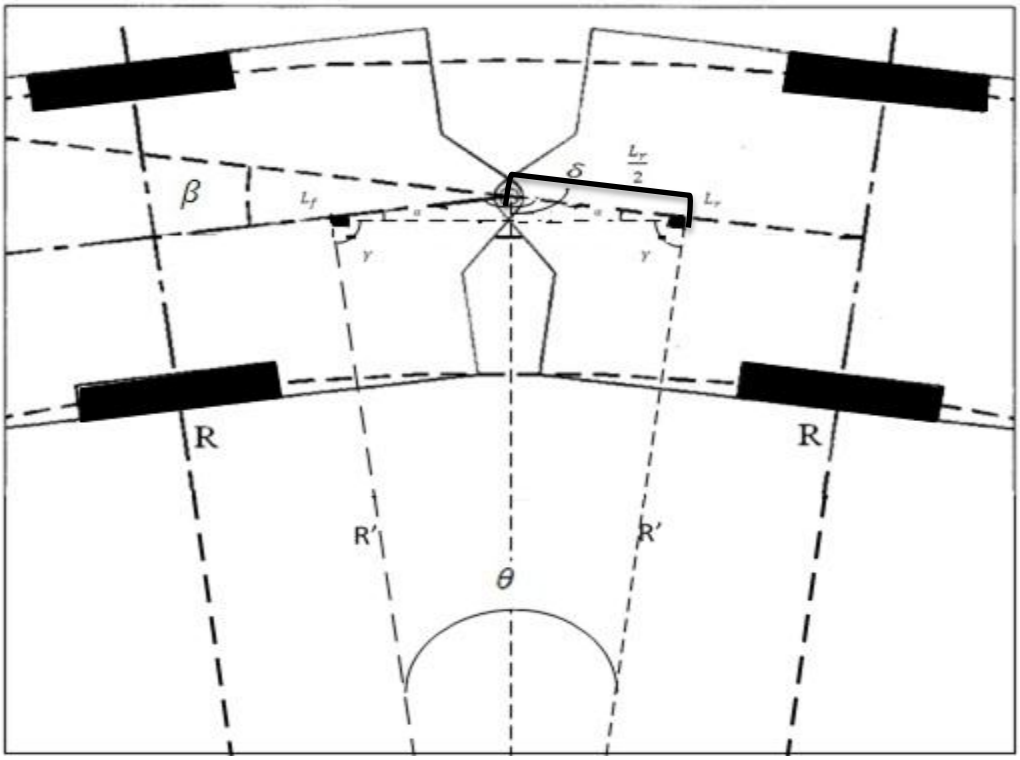

Figure 39: A detail of turning radius calculation

$$\begin{cases} R'.sin\frac{\theta}{2} = F \\ \frac{L_r}{2}.cos\alpha = F \\ \beta = 2\alpha \\ R'.sin\frac{\theta}{2} = \frac{L_r}{2}.cos\alpha \\ R' = \frac{L_r}{2}.cot\frac{\beta}{2} \end{cases} \quad (4.4)$$

And according to the Thales theorem the articulation radius is:

$$R = L_r.cot\frac{\beta}{2} \quad (4.5)$$

This result confirms that there is a direct relation between the amount of steering angle and articulation radius of the machine. It is also depended on the amount of front or rear axis length.

Chapter 5

5.0 Simulation results and discussion

The results from various testing are presented and discussed in this section. The open loop controller's response is compared with the closed loop controller's response and the machine is tested in different conditions. The comparison between Velocity, pump volumetric displacement and differential pressure over pump is done. The Figure 40 shows the machine's test terrain and the field in front of the Hydraulic lab. The graphical model of the terrain simulates the surrounding environment of the lab with details which exists in the area.

Figure 40: The graphical model of the terrain

5.1 Results of Simulation without external load

The Machine is tested on a flat surface and on a straight line. As the figure 41 shows the velocity of the IHA machine is compared between the open loop controller's response and the closed loop controller's response. The desired velocity is being sent to the system after passing through a low pass filter.

The transfer function of the low pass filter is F= $\frac{1}{0.3s+1}$

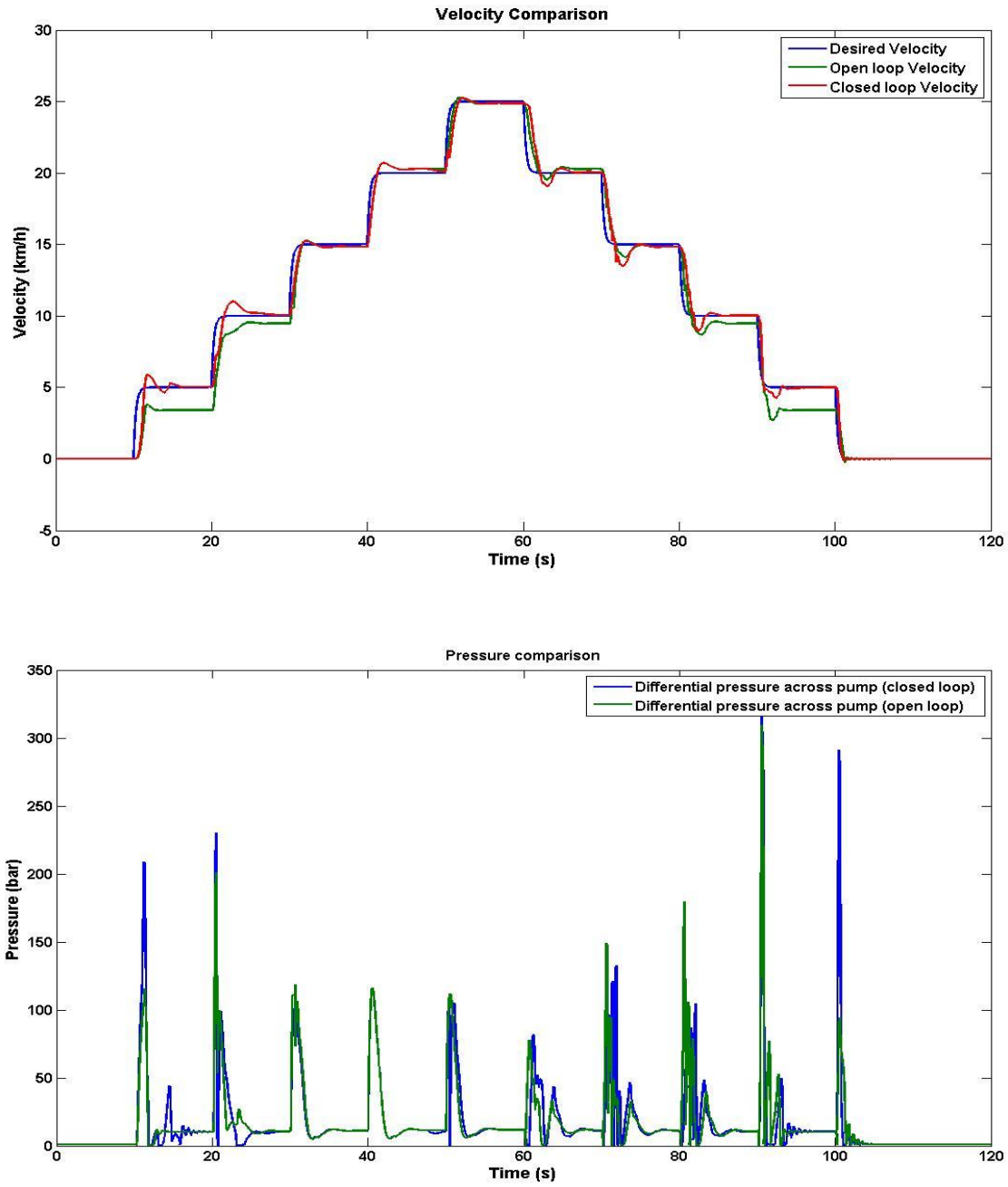

Figure 41: Comparison between the open loop and closed loop velocity & pressure over the main hydraulic pump, test on the horizontal plane

The closed loop response is following the desired velocity more accurate than the open loop response. There is an overshoot around 5.87 % in the closed loop response in low speed. There is a tracking error about 1.5 (km/h) between the desired velocity and the measured velocity in the open loop response in low speed. The maximum speed that the machine can reach is about 25 (km/h) with full volumetric displacement of hydraulic motor. If the volumetric displacement of the hydraulic motor changes to its

half the maximum speed can become 50 (km/h). The pressure picks in the figure 41 show the time when the machine starts to accelerate or decelerate. Since the machine is moving on a smooth terrain, the pressure gets back to its minimum after acceleration or deceleration. The minimum of differential pressure across the main pump is 20 Bar and the maximum pressure is limited to 350 Bar.

5.2 Results of the simulation with external disturbance

In this section the external disturbance is defined as the gravity force which effects on the performance of the machine when it enters a ramp. The figure 42 shows where the ramp starts and when it stops.

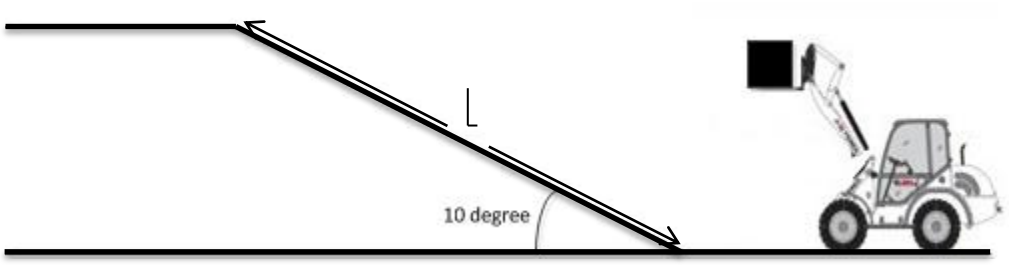

Figure 42: the ramp

The other types of disturbance like air drag force, hydraulic works in actuators & etc. is not considered. The machine is tested on a gradient terrain with length (L) of 90 m. The maximum slop of terrain where the machine can cross over it is considered to be 10 degree.

The figure 43 shows the comparison of velocity between the closed loop and open loop controller's responses.

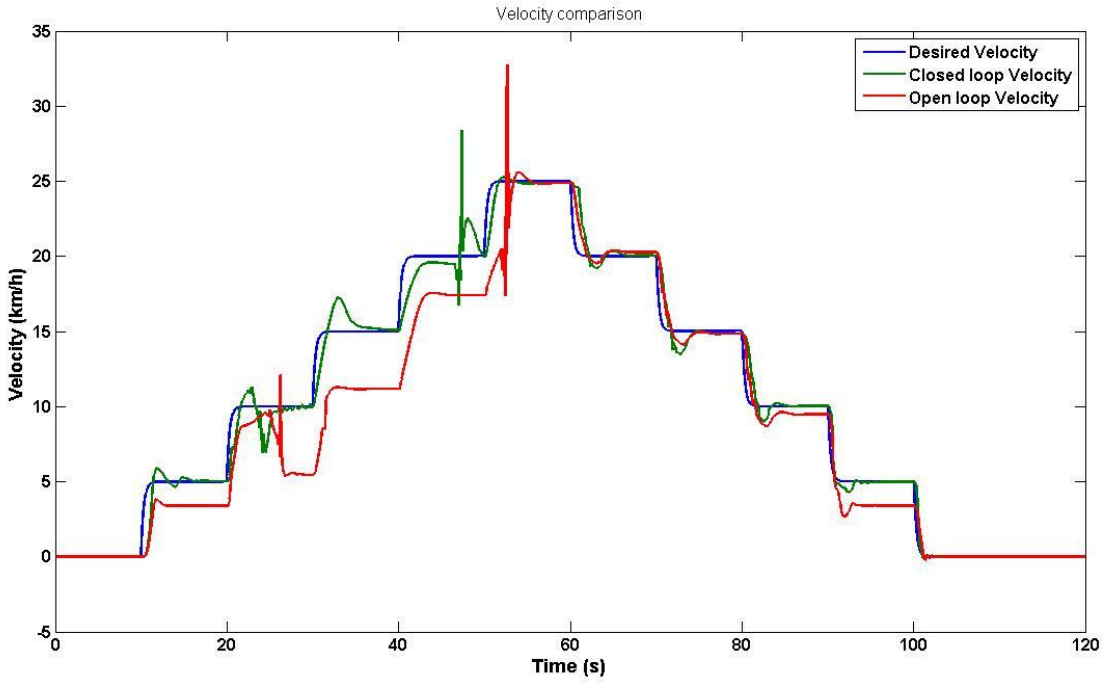

Figure 43: comparison of velocity between the closed loop & open loop responses, test on the ramp

The closed loop response follows the desired velocity more accurate than the open loop response.

The machine is tested once with the open loop controller and then with closed loop controller. The machine with open loop & closed loop controllers starts the track from the same location.

The machine with closed loop control can finish the ramp in 25 s but the machine with open loop control does it in 29 s. this four second is the reason of time difference between the spikes at the beginning & end of the ramp. And because the speed is smaller in open loop case there is such a time difference.

The figure 44 shows the hydraulic pump volumetric displacement comparison between the closed loop and open loop controllers.

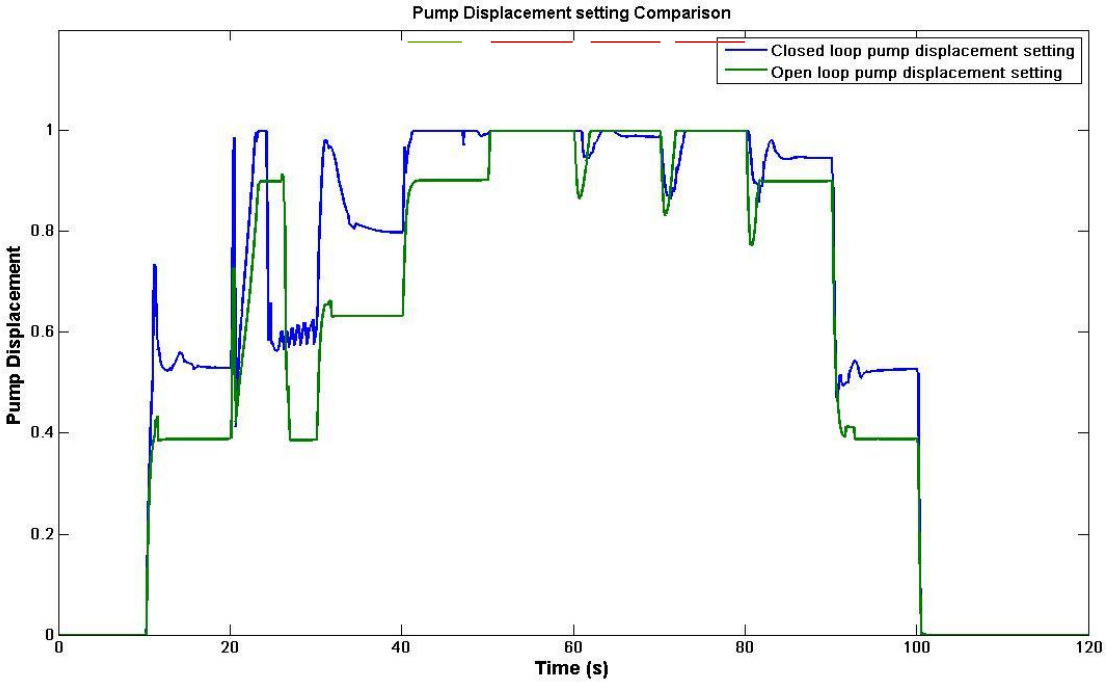

Figure 44: hydraulic pump volumetric displacement comparison, test on the ramp

As the figure 44 shows most of the times the pump volumetric displacement's value in closed loop control is higher than the open loop. This figure demonstrates that how the feedback controller tries to compensate the error by modification of pump displacement setting as a manipulated variable.

The figure 45 shows the comparison of pressure across the main hydraulic pump and between the closed loop and the open loop controller.

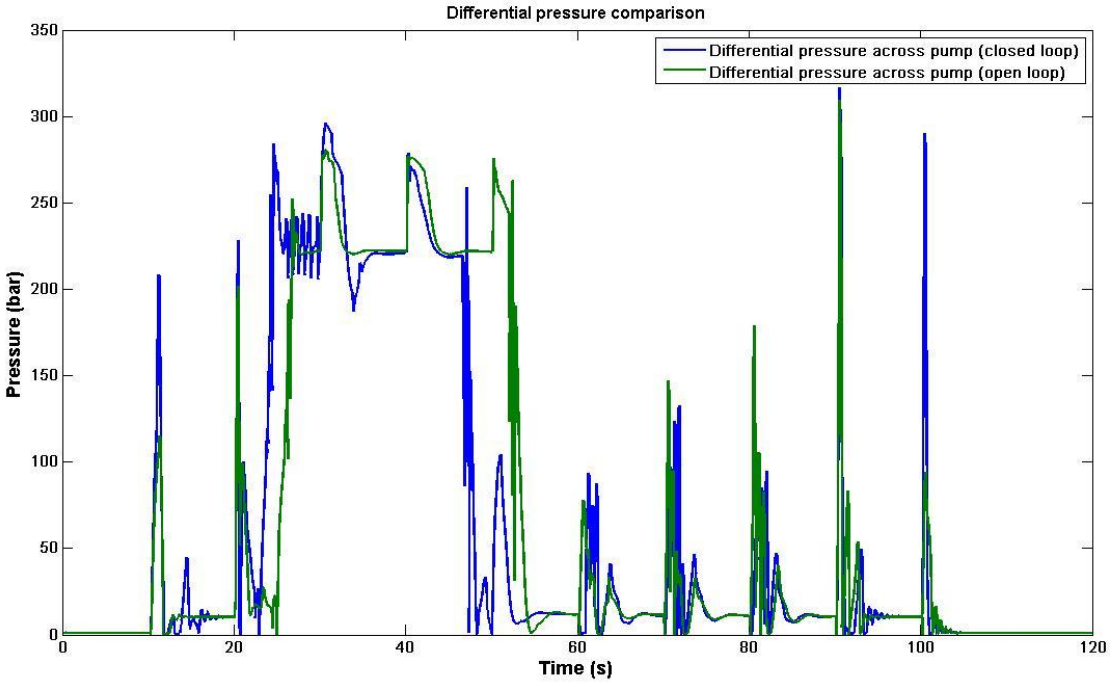

Figure 45: comparison of pressure over the main hydraulic pump, test on the ramp

When the machine enters the ramp the pressure difference across the main pump gets close to the maximum and when the slop of the terrain becomes zero the differential pressure drops to its minimum. When the machine enters the ramp at 23s the closed loop differential pressure (blue curve) rises faster than the open loop pressure (green curve) and the pressure drops faster when the ramp ends.

5.3 Conclusion

IHAkone is an articulated-frame-steering mobile machine powered by a diesel engine. The engine rotates a variable displacement pump, which is turn provides fluid pressure to four parallel fixed displacement motors which rotate the wheels. In our modeling, we consider hydro-mechanical and volumetric efficiencies. These efficiencies are parameters of operating conditions which are pressures and rotation speeds. We then design control laws for machine speed control in a feedback/feed forward configuration. Model is linearized in several nominal operating conditions, for each of which a PID controller is designed. The gain scheduling of PID controller is based on the rotation speed of hydraulic motors which is readily available from wheel encoders.

There are two manipulated variable which can effect on the speed of the machine: 1)- diesel engine rotational velocity (RPM); 2)- volumetric displacement of the pump. Speed of the machine is proportional to product of these two variables, in steady state. Based on efficiency curves of power transmission components and diesel engine and their operating limits, a power optimization algorithm calculates desired values for RPM and displacement of the pump. Because of model uncertainties (on which power optimization algorithms are based), open loop use of this variables will result in inaccurate speed tracking performance. In our control strategy, we directly send the desired RPM values to the servo controller of the diesel engine. However, the desired displacement is first corrected using a feedback control law before sending to the pump. The feedback controller receives the desired speed of the machine. Experiments show that feedback alone is not enough to cancel all the tracking errors, especially in high loads, for example when entering to a ramp. A feed-forward term is used to eliminate the transient tracking error. Terrain slope is used to calculate the feed-forward signal. This value is essentially the pitch angle of the machine provided by a tilt sensor or an IMU (Inertial Measurement Unit).

According to the strategy taken in the optimization unit to reduce the fuel consumption, the diesel engine RPM is kept as low as possible and volumetric displacement of the pump as high as possible. There is a time delay about 2-3 seconds to increase the diesel engine (RPM) to produce enough output power when the machine enters the ramp. Notice that feedback/feed-forward controller manipulates the pump displacement, and when this variable is in maximum (1 or 100%), the control becomes open-loop and feed forward signal has no effects.

With slop higher than 10 degree may cause the machine to stop completely for a short time especially if the machine is moving with a low velocity. Using a predictive control, we can eliminate such poor transition. For that, we need to gather knowledge about the gradient of the terrain ahead of us. For such predictive control knowledge about the upcoming terrain is essential. IHAkone is equipped with environmental sensors to map the surroundings (Laser scanners for example) which can be used to this purpose.

6 References

[1] Aström, K.;Control System Design. Preprint.

[2] Backas, J.,Ahopelto, M.,Huova, M.,Vuohijoki, A,Karhu, O.,Ghabcheloo, R & Huhtala, K.; IHA-Machine A future Mobile Machine. The Twelfth Scandinavian International Conference on Fluid Power, May 18-20, 2011, Tampere, Finland.

[3] Belanger, P. R. (1995). Control Engineering A Modern Approach. New York: Oxford University Press.

[4] Bulletin 0274-B1, Mobile Hydraulic Technology, Parker mobile hydraulic,1999.

[5] Dorf, R and Bishop, R; Modern control systems, Ninth edition, Prentice Hall, 2001.

[6] Franklin F., Powel J., Emami A.; Feedback Control of Dynamic Systems, 4th edition, Pearson Education, 2002.

[7] Ghabcheloo, R. and Hyvönen, M. "Odometry and motion control of an articulated-frame-steering hydraulic mobile machine," submitted to 48th IEEE Conference on Decision and Control and 28th Chinese Control Conference. Shanghai, China. Dec. 2009.

[8] Ghabcheloo, R., Hyvönen, M., Vuohijoki, A., Huhtala, K., & Matti, V. (2009). NEW STEERING MECHANISM AND HYDROSTATIC TRANSMISSION SYSTEM FOR ARTICULATED-FRAME-STEERING MOBILE MACHINES.The 11th Scandinavian International Conference on Fluid Power, SICFP'09, Linköping.

[9] Ghabcheloo, R., Hyvönen, M., Uusisalo, J., Karhu, O., Järä, J., and Huhtala, K., "Autonomous motion control of a wheel loader," submitted to ASME Dynamic Systems and Control Conference and Bath/ASME Symposium on Fluid Power & Motion Control, Hollywood, CA. Oct. 2009.

[10] Ghabcheloo, R., & Hyvönen, M. (2009).Modeling and motion control of an articulated-frame - steering hydraulic mobile machine. 17th Mediterranean Conference on Control and Automation, MED'09, Greece.

[11] Gosal, A. S. (2004, August). Modeling and Control of a Hydrostatic Transmission for a Load-Haul-Dump Underground-Mining Machine. Vancouver, Canada.

[12] HUHTALA, K; Modeling of Hydrostatic Transmission-Steady State, Linear and Non-Linear Models, Acta polytechnic Scandinavia, Mechanical engineering series, No 123,Helsinki 1996.

[13] Huhtala,K., Suomela, J., Vilenius, M. and Halme, A.2008. Toward intelligent mobile machines-GIM research. Fluid Power and Motion Control FPMC 2008, September 10-12, Bath, UK.pp.277-290.

[14] Hyvönen M., Vilenius J., Vuohijoki A., and Huhtala K., "Mathematical Model of the Valve Controlled Skid Steered Mobile Machine," 2nd International Conference on Computational Methods in Fluid Power, August 2006, Aalborg, Denmark.

[15] Merritt, H; Hydraulic Control Systems, second edition, JOHN WILEY & SONS, 1967.

[16] Manring, N, Hydraulic control systems, first edition, JOHN WILEY & SONS, 2005.

[17] Pacejka, H. Tyre and Vehicle Dynamics . Bodmin, Cornwall, UK: MPG Books Ltd.

[18] RAJAMANI, R; Vehicle Dynamics and Control.Springer,2006.

[19] Vilenius J. "Characteristics of Valve Controlled Hydraulic Power Transmission in Teleoperated Skid Steered Mobile Machine" Dissertation NO 654, Tampere University of Technology, 2007.

Appendix A

Simulink Models:

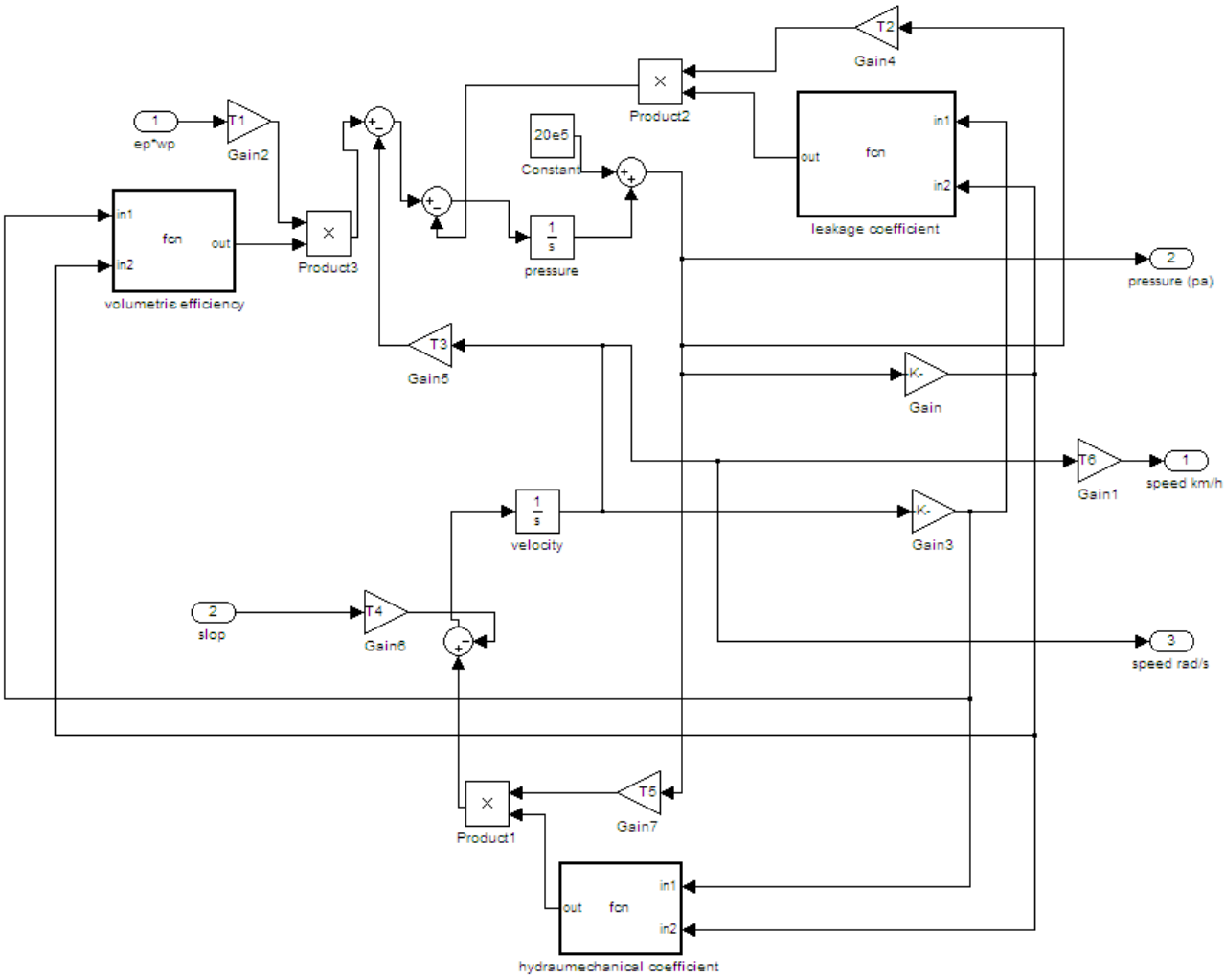

Figure (A.1): HST & body model

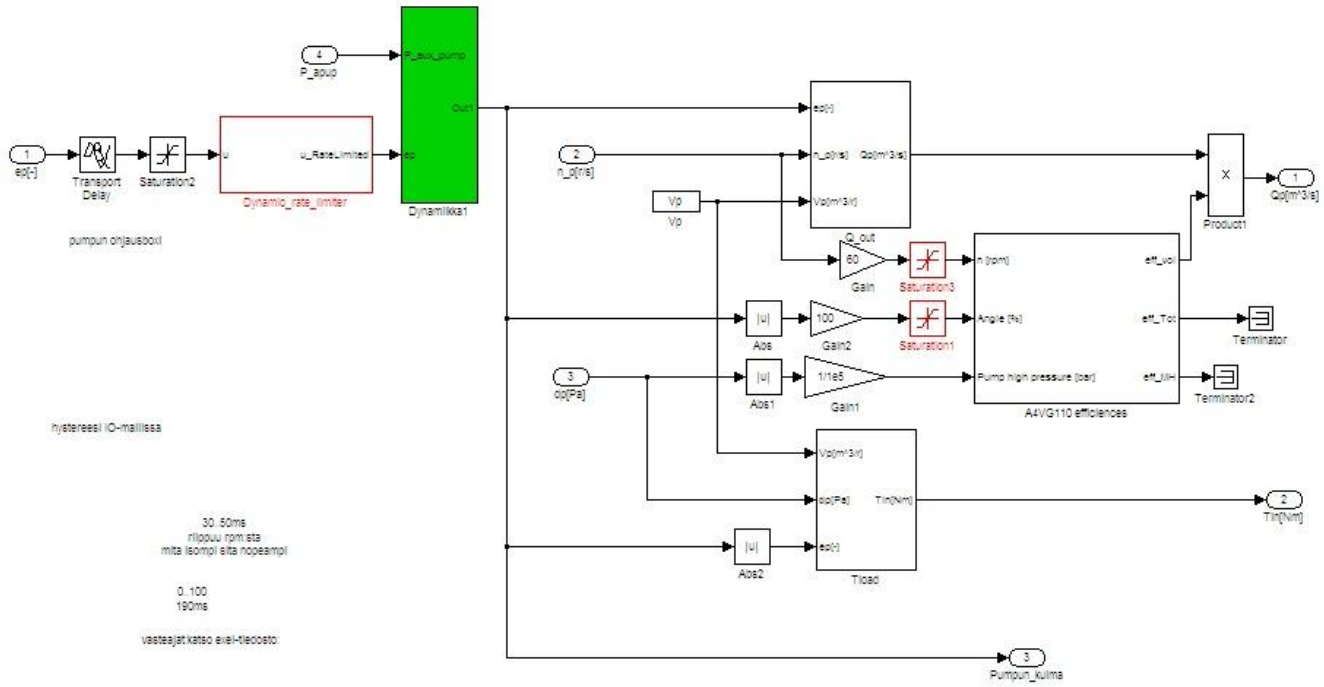

Figure (A.2): Hydraulic Pump Model

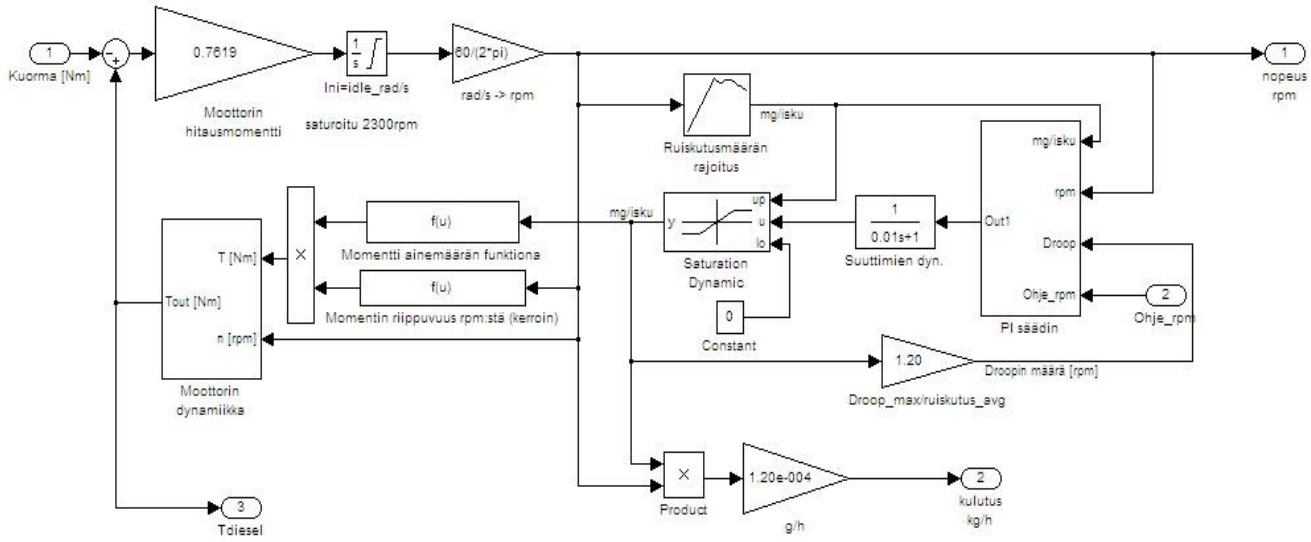

Figure (A.3): Diesel Engine model

Appendix B:

.m files:

This appendix includes the m.file which defines the volumetric and mechanical efficiencies of the pump and motor and also the leakage coefficient. The modification of these efficiencies can change the dynamic characteristic of the model.

Leakage coefficient modification:

```
function out = fcn(in1,in2)


if ((in1 >= -5) && (in1 <= 25))
   if ((in2 >= 0) && (in2 <= 100))
      out = 2.1730*10^(-11);
   elseif ((in2 > 100) && (in2 <= 200))
      out = 1.4819*10^(-11);
   elseif ((in2 > 200) && (in2 <= 300))
      out = 1.2208*10^(-11);
   else
      out = 1.0707*10^(-11);
   end
elseif ((in1 > 25) && (in1 <= 50))
   if ((in2 >= 0) && (in2 <= 100))
      out = 3.8861*10^(-11);
   elseif ((in2 > 100) && (in2 <= 200))
      out = 2.9737*10^(-11);
   elseif ((in2 > 200) && (in2 <= 300))
      out = 2.4793*10^(-11);
   else
      out = 2.2091*10^(-11);
   end
elseif ((in1 > 50) && (in1 <= 100))
   if ((in2 >= 0) && (in2 <= 100))
      out = 3.8250*10^(-11);
   elseif ((in2 > 100) && (in2 <= 200))
      out = 3.0347*10^(-11);
   elseif ((in2 > 200) && (in2 <= 300))
      out = 2.5235*10^(-11);
   else
      out = 2.3426*10^(-11);
   end
else
   out = 2.1730*10^(-11);
end
```

Volumetric efficiency of the pump modification:

```
function out = fcn(in1,in2)

%#eml

if ((in1 >= 0) && (in1 <= 25))
   if ((in2 >= -5) && (in2 <= 100))
      out = 0.4572;
   elseif ((in2 > 100) && (in2 <= 200))
      out = 0.5009;
   elseif ((in2 > 200) && (in2 <= 300))
      out = 0.4317;
   else
      out = 0.4155;
   end
elseif ((in1 > 25) && (in1 <= 50))
   if ((in2 >= 0) && (in2 <= 100))
      out = 0.650;
   elseif ((in2 > 100) && (in2 <= 200))
      out = 0.7088;
   elseif ((in2 > 200) && (in2 <= 300))
      out = 0.5801;
   else
      out = 0.5582;
   end
elseif ((in1 > 50) && (in1 <= 100))
   if ((in2 >= 0) && (in2 <= 100))
      out = 0.800;
   elseif ((in2 > 100) && (in2 <= 200))
      out = 0.84;
   elseif ((in2 > 200) && (in2 <= 300))
      out = 0.75;
   else
      out = 0.73;
   end
else
   out = 0.98;
end
```

Hydro mechanical efficiency of the motor:

```
function out = fcn(in1,in2)

%#eml

if ((in1 >= -5) && (in1 <= 25))
   if ((in2 >= 0) && (in2 <= 100))
      out = 0.66;
   elseif ((in2 > 100) && (in2 <= 200))
      out = 0.7;
   elseif ((in2 > 200) && (in2 <= 300))
      out = 0.74;
   else
      out = 0.76;
   end
elseif ((in1 > 25) && (in1 <= 50))
   if ((in2 >= 0) && (in2 <= 100))
      out = 0.845;
   elseif ((in2 > 100) && (in2 <= 200))
      out = 0.8675;
   elseif ((in2 > 200) && (in2 <= 300))
      out = 0.885;
   else
      out = 0.895;
   end
elseif ((in1 > 50) && (in1 <= 100))
   if ((in2 >= 0) && (in2 <= 100))
      out = 0.8712;
   elseif ((in2 > 100) && (in2 <= 200))
      out = 0.8989;
   elseif ((in2 > 200) && (in2 <= 300))
      out = 0.9161;
   else
      out = 0.9184;
   end
else
   out = 0.66;
end
```

Appendix C:

Oscillation and tracking error

Power management of a mobile machine, in its simplest form, allocates available diesel power to different consumers (drive, steering, and work hyd.). The decision is made based on power request of each user, power or torque curves. Needed power for drive, for example, is decided base on pressure measurements and speed command. Use of pressure measurements for this calculation make a feedback loop, which in certain operating points becomes unstable and cause oscillation. We have proposed a method to prevent the instability in the system by using low pass filters in the feedback loop. The figure C.1 shows where the filters are located.

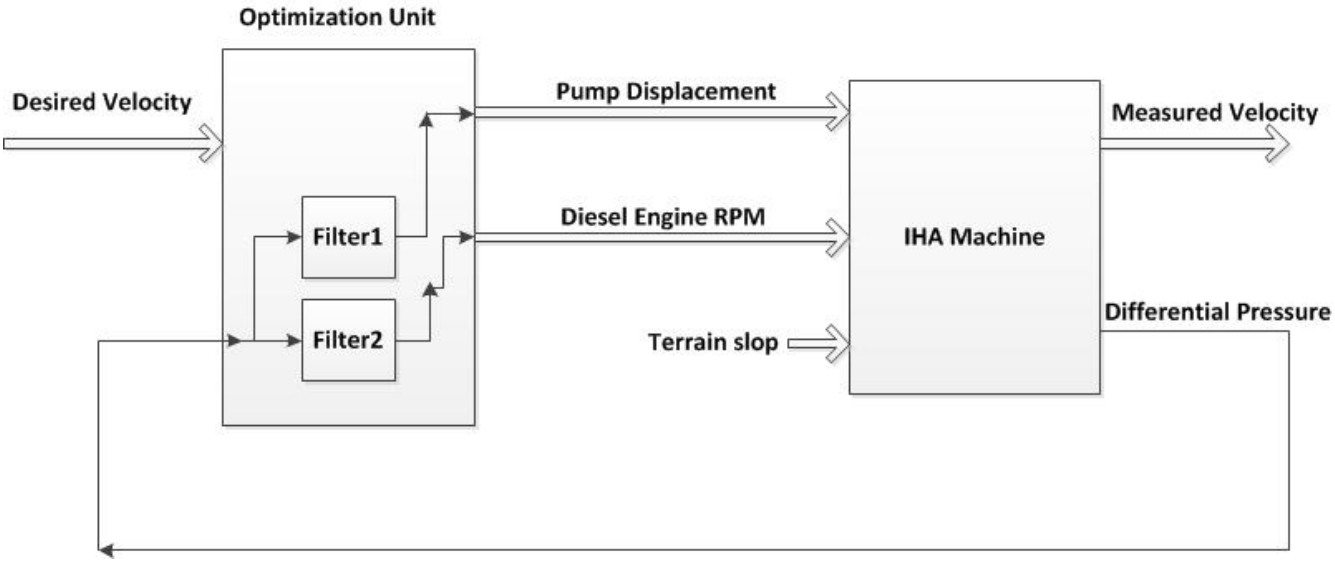

Figure C.1: the pressured based feedback loop

The problem of oscillation originates from the speed and torque control block and the possible solution to remove the oscillation is using a low pass filter with the possibility of switching. The structure of the system is presented in the figure C.2 where P1(s) is the transfer function of machine, P2(s) is the transfer function of slop as input and differential pressure as output, p3(s) is the transfer function of differential pressure as input and velocity as output, K2(s) is the transfer function of pressure as input and diesel engine rpm as output, K3(s) is the transfer function of pressure as input and pump displacement setting as output, VOL(s) is the transfer function of pressure as input and volumetric efficiency of pump as output, MH(s) is the transfer function of pressure as input and mechanical efficiency of motor as output and K1(s) is the inverse of P1(s).

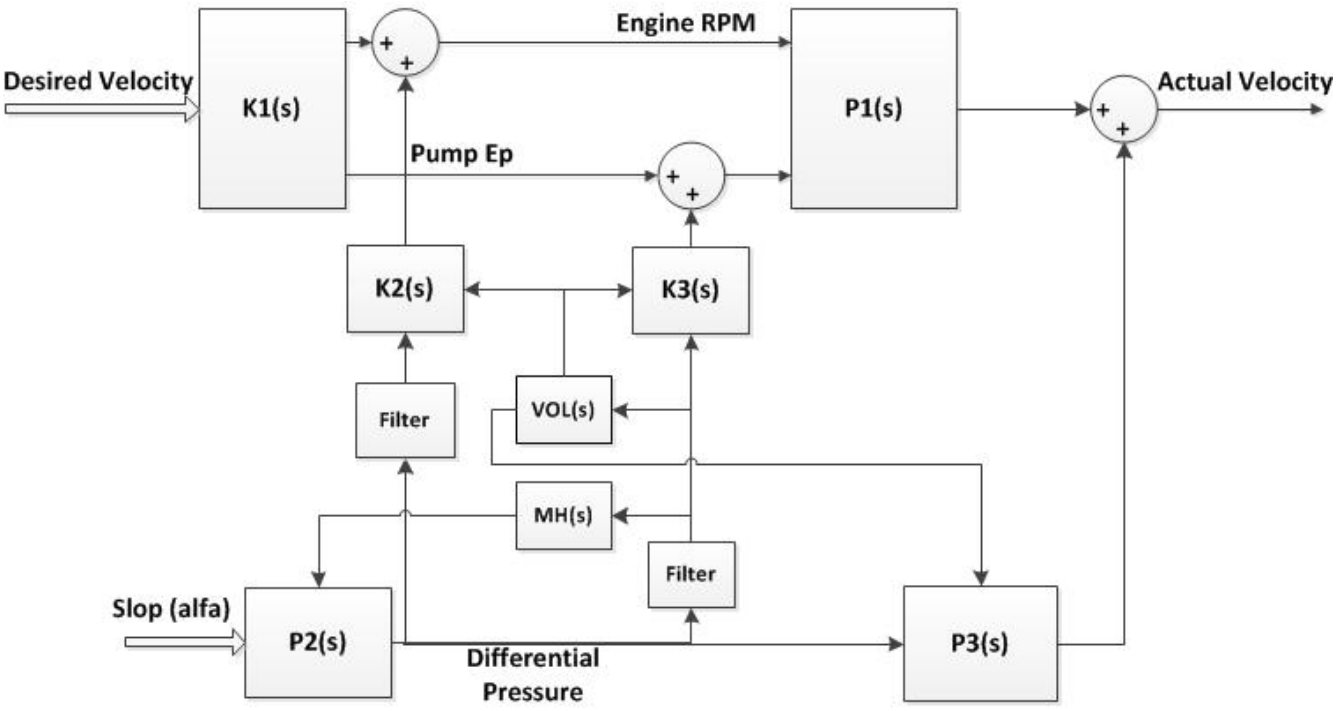

Figure C.2: The effect of differential pressure on velocity with details

As the Figure C.2 shows two different low pass filter are used for differential pressure Δp which is a state variable of the system. The discrete transfer function of the filter for pump is

G1(s)= 0.00554/(z-0.9945) and the transfer function of the filter for engine is G2(s)= 0.2212/(z-0.7788). The effect of the filter is to make the system more damped and it increases the time delay in the system's response. Differential pressure is one of the parameters which can modify the pump displacement setting and diesel engine rpm values in the power management unit. The pressure is filtered for **efficiency_model1** and **Driving_Pump_Angle** and **Diesel_Requirements_Driving** blocks with one distinction that the filter of diesel engine will be activated when the differential pressure gets to 200 bar pressure. The reason behind the switching of filtering for diesel engine is to prevent the engine to stall when the machine enters a ramp.

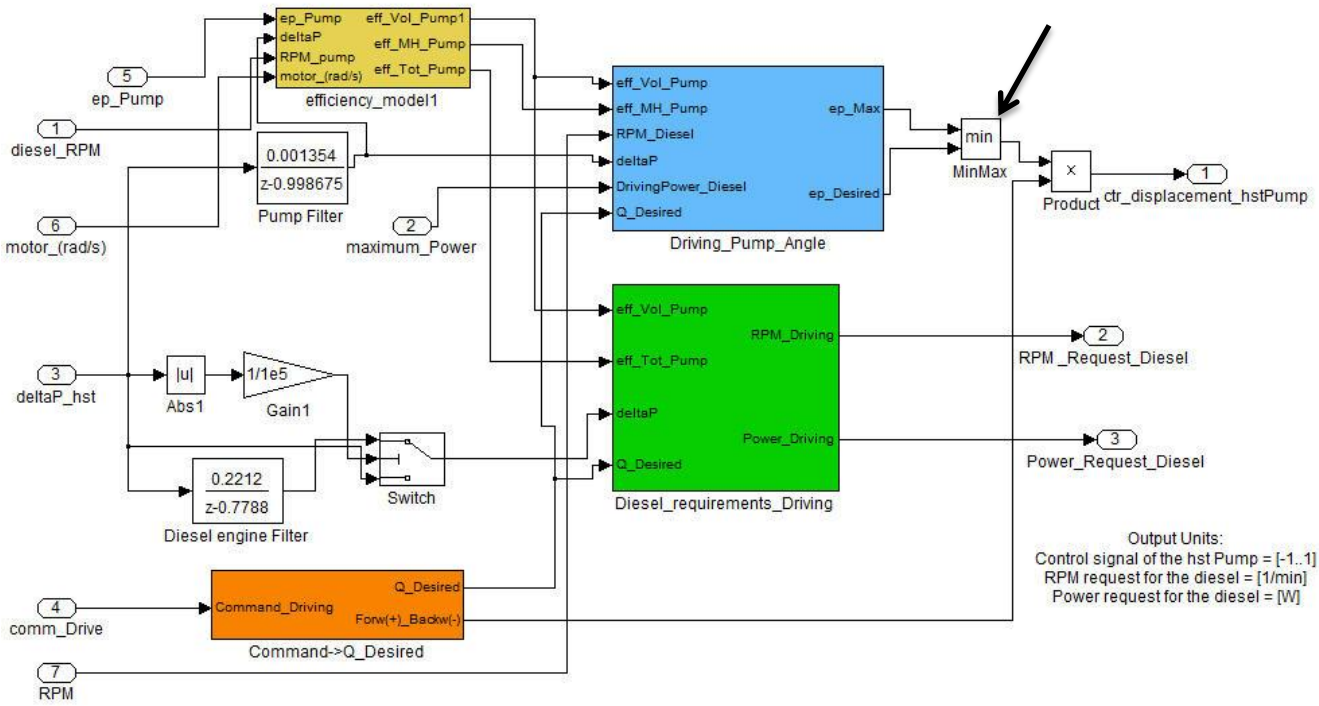

Figure C.3: Original speed and torque control block in Simulink model

The problem of tracking error originates from the calculation problem of the machine's inverse dynamic model in the open loop controller. The volumetric and hydro mechanical efficiencies of pump and motors have non-linear behavior and they are dependent on differential pressure, pump displacement and diesel engine rpm as explained before. So the estimated linear efficiency's values of pump and leakage coefficient of motor can cause inaccuracy in the calculated inverse dynamic model of the system in open loop controller. The inaccuracy can lead to the speed tracking error in the open loop controller. The open loop controller **(optimization block)** calculates the required pump displacement setting and diesel engine rpm for a desired velocity, however as we mentioned earlier due to nonlinearity of efficiencies the calculated inverse dynamic model in the optimization block is not precise and it may cause speed tracking error. The problem can be resolved by using the speed feedback control.

There is another way to prevent oscillation in the system by removing the minimizer block as shown in the figure C.3 and connecting the calculated desired pump displacement setting to the product block. This method is used in all the simulation parts in the thesis and the oscillation is eliminated from the results, however in practice the diesel engine may stall with this method in high pressure picks. Therefore the possible way to remove the oscillation from the system is using the low pass filtering.